

Comparison of Traditional Image Segmentation Techniques and Geostatistical Threshold

Matthew Kerwin, B.Sc(CompSci)

Supervisor: Assoc. Prof. Tuan Pham

04 July 2006

School of I.T, Maths & Physics

James Cook University

Townsville, Australia

Dissertation submitted by Matthew Kerwin in partial fulfillment of the requirements for the Degree of
Bachelor of Science with Honours in the Department of Computer Science at James Cook University.

Declaration

I declare that this thesis is my own work and has not been submitted in any form for another degree or diploma at any university or other institute of tertiary education. Information derived from the published and unpublished work of others has been acknowledged in the text and a list of references is given.

Date

Abstract

A general introduction to image segmentation is provided, including a detailed description of common classic techniques: Otsu's threshold, k -means and fuzzy c -means clustering; and suggestions of ways in which these techniques have been subsequently modified for special situations.

Additionally, a relatively new approach is described, which attempts to address certain exposed failings of the classic techniques listed by incorporating a spatial statistical analysis technique commonly used in geological studies.

Results of different segmentation techniques are calculated for various images, and evaluated and compared, with deficiencies explained and suggestions for improvements made.

Acknowledgements and Dedication

Thanks to my supervisor, Associate Professor Tuan Pham, for taking me on and telling me to ‘sleep less’. Thanks also to Dr. Bruce Litow for taking a risk and offering me a position. And of course, many thanks to my lovely wife Rochelle for putting up with my extended tour as a student when I should have been out earning money.

For Fidget

Contents

List of Tables	iii
List of Figures	iv
1 Introduction	1
1.1 Image Segmentation	1
1.2 Current Techniques	2
1.2.1 Otsu’s Thresholding Method	5
1.2.2 k -Means Clustering	7
1.2.3 Fuzzy c -Means Clustering	10
1.3 Shortcomings of Otsu, k -Means and Fuzzy c -Means for Image Segmentation	12
2 Geostatistical Threshold	15
2.1 Geostatistics	15
2.2 Experimental Semivariogram	16
2.3 Geostatistical Threshold	18
3 Experiments	20
3.1 Images	20
3.2 Techniques	21

4	Results and Discussions	24
4.1	Discussions	63
5	Conclusions	64
5.1	Suggestions for Further Research	65
	Bibliography	67

List of Tables

4.1 Results	62
-----------------------	----

List of Figures

1.1	Images With Identical Histograms	13
3.1	Retinal Image	23
4.1	Nodules	25
4.2	Fluorescene Cells A	27
4.3	Fluorescene Cells B	28
4.4	Fluorescene Cells C	29
4.5	Fluorescene Cells D	30
4.6	Fluorescene Cells E	31
4.7	Fluorescene Cells E (detail)	32
4.8	Cell Clusters 1	33
4.9	Cell Clusters 2	34
4.10	Cell Clusters 3	35
4.11	Cell Clusters 3 (cropped)	36
4.12	Cell Clusters 4	37
4.13	Cell Clusters 4 (detail)	38
4.14	Cell Clusters 5	39
4.15	Cell Clusters 5 (cropped)	40
4.16	Cell Clusters 6	41
4.17	Cell Clusters 6 (cropped 1)	42

4.18 Cell Clusters 6 (cropped 2)	43
4.19 Cell Clusters 7	44
4.20 Cell Clusters 7 (cropped)	45
4.21 Cell Clusters 8	46
4.22 Cell Clusters 8 (cropped 1)	47
4.23 Cell Clusters 8 (cropped 2)	48
4.24 Cell Clusters 9	49
4.25 Cell Clusters 9 (cropped 1)	50
4.26 Cell Clusters 9 (cropped 2)	51
4.27 Cell Clusters 10	52
4.28 Cell Clusters 10 (cropped)	53
4.29 Helicopter	56
4.30 Retinal Image 1	57
4.31 Retinal Image 2	58
4.32 Retinal Image 3	59
4.33 Retinal Image 4	60
4.34 Retinal Image 5	61

Chapter 1

Introduction

This document aims to provide a general background to image segmentation: describing and comparing some classical techniques, looking at ways in which other researchers have adapted them to specific problems, and suggesting further reading on those specialisations as well as other techniques used in image segmentation.

It provides a detailed explanation of a recently implemented technique, highlighting a particular area of study that may provide an improvement over existing techniques by combining knowledge from other fields of scientific research, in this case geology.

1.1 Image Segmentation

Image segmentation is the process by which an image is divided into regions, or segments, based on various criteria. Greyscale Image Segmentation is a form of image segmentation whereby a two-dimensional image is divided

into two segments — foreground and background — according to some relationship of the pixels’ *intensity* or *grey* levels. The resulting segmentation can be interpreted as a monochrome (black and white) image, where either black or white pixels are designated as foreground, and the remainder as background. Foreground pixels can be said to be ‘interesting’, in that they represent some object or feature which is of interest to study; background pixels are ‘uninteresting’ as they provide no immediate value for analysis.

Image segmentation is useful in any context where an image (such as a photograph) is to be in any way analysed automatically by a computer. Of particular interest are applications in bioinformatics, such as: assisted diagnosis of diabetic retinopathy by analysing retinal scan images [1, 2, 3]; studies of treatments on cell populations, by analysing changes in size, shape, or numbers of cells; and assisted analysis of Magnetic Resonance Image scans to diagnose any number of pathologies [17, 12, 13]. By automating even part of the process, a *triage* system is implemented whereby the computer is able to determine at high speed which cases are healthy, and which require more attention from a doctor. By performing the initial diagnosis at high speed, eliminating unnecessary cases, and highlighting particular areas of concern, the workload of the diagnosing doctor is significantly reduced, allowing a much larger body of data to be studied with the same level of detail in less time.

1.2 Current Techniques

Currently various approaches to image segmentation are used, of which I will describe some of the most well-established and recognised below. When categorising image segmentation techniques it is useful to refer to the underlying

process each technique uses.

The simplest greyscale segmentation approach to comprehend is that of thresholding, which involves defining a particular intensity value as a threshold such that any pixel with an intensity greater than the threshold is labelled ‘white’, and any less than or equal to the threshold is labelled ‘black’. Then, depending on the particular image and context, either ‘black’ or ‘white’ pixels are said to be foreground, and the others background. One commonly used and well recognised thresholding technique, proposed by Nobuyuki Otsu in 1978[4], explained in detail in section 1.2.1, uses statistical analysis of the image’s grey-level histogram to determine the optimal threshold. Other thresholding techniques have been suggested which use different objective functions to evaluate the optimality of a threshold. For example, by using techniques made available through fuzzy set theory, a threshold may be evaluated by some measure of fuzziness[5] of the resulting partitioned image, such as the linear index of fuzziness[6], fuzzy entropy[7] or fuzzy correlation. All these techniques follow the same basic approach as Otsu’s threshold, with variations in the details of implementation, in particular the objective function used to evaluate a threshold. As such, a detailed explanation of Otsu’s threshold will be provided, along with explanations of where the algorithm may be altered to incorporate different suggested techniques.

Many image thresholding techniques are described in detail by Chi *et. al.* [8, pp. 45-84], with examples of applications of different techniques.

Another common approach to greyscale image segmentation uses clustering techniques to group pixels according to common characteristics. One such technique, known as k -means clustering, is a fixed-class-number variant of the ISODATA technique[9], which uses a recursive approach to classify pix-

els into classes and optimise that classification. In terms of greyscale image segmentation, the number of classes used in k -means is fixed at 2 (foreground and background). A fuzzy generalisation of k -means, proposed initially by Dunn in 1973[10] then improved upon by Bezdek in 1979[11], is known as fuzzy c -means (FCM). Both k -means and FCM will be explained in detail in sections 1.2.2 and 1.2.3 respectively. These techniques, particularly FCM, are widely studied and various attempts have been made to improve their functionality in various special situations[12, 13, 14, 15, 16, 17], however this document will focus only on the original and basic forms of the algorithms, and will provide suggestions of further reading on subsequent techniques.

More recently various different approaches to greyscale image segmentation have been proposed. One such technique, for example, is *region growing*, whereby some method is used to choose a seed point in the image (typically this is performed manually by an operator, who selects a set of ‘interesting’ pixels), and the algorithm extracts all pixels connected to the initial seeds based on some predefined criteria, such as until an edge is detected in the image. Documents discussing region growing, as well as other general approaches to image segmentation (such as using classifiers, Markov random field models, artificial neural networks, deformable models, and atlas-guided approaches) are provided elsewhere[18, 29].

It has also been suggested that a fuzzy rule-based approach may be used in image segmentation, by interpreting image features as linguistic variables[19] and using fuzzy *if-then* rules to segment an image into regions. Descriptions of fuzzy rule-based systems are provided by Chi *et. al.*[8, 139-187], however a study of available literature suggests that this approach is not commonly utilised in contemporary research, and Chi *et. al.* describe inherent difficulties

and problems with the approach[8, pg. 186], and as such fuzzy rule-based systems will not be studied in detail in this document.

1.2.1 Otsu’s Thresholding Method

The simplest greyscale image segmentation technique to comprehend is segmentation by thresholding. A threshold is an intensity value which is used as the boundary between the two classes of a binary segmented image. One approach, proposed by Otsu in 1978[4], attempts to create a measure of “goodness” or optimality of a threshold using statistical analysis, which can be used to determine the optimal threshold for an image. The threshold which results in the best separation of classes is considered to be optimal. Class separation is described in terms of statistical analysis as either high *between-class variance*, low *within-class variance*, or a combination of both.

The process requires iteratively evaluating all possible thresholds, to eventually determine the optimum. As such, discrete threshold values are required, a situation ideally suited to traditional bitmap images, in which each pixel describes a discrete intensity value.

Given an image X , made up of N pixels, $(x_j, j = 1, \dots, N)$ with intensity values from $R = (1, 2, \dots, L) \subset \mathcal{Z}$, we say that the probability distribution of intensity value $i \in R$ in X is:

$$p_i = \frac{n_i}{N}, \quad p_i \geq 0, \quad \sum_{i=1}^L p_i = 1 \quad (1.1)$$

That is, the number of pixels with intensity value i divided by the total number of pixels. Then, given that the image is to be divided into two classes c_0 and c_1 with a threshold at level k such that c_0 denotes pixels with levels $[1, \dots, k]$, and c_1 denotes pixels with levels $[k + 1, \dots, L]$, the probabilities of

class occurrence (the odds that a randomly chosen pixel will be of a particular class) and the class mean levels, respectively, are given by:

$$\omega_0 = \Pr(c_0) = \sum_{i=1}^k p_i = \omega(k) \quad (1.2)$$

$$\omega_1 = \Pr(c_1) = \sum_{i=k+1}^L p_i = 1 - \omega(k) \quad (1.3)$$

and

$$\mu_0 = \sum_{i=1}^k i \Pr(i|c_0) = \sum_{i=1}^k \frac{ip_i}{\omega_0} = \frac{\mu(k)}{\omega(k)} \quad (1.4)$$

$$\mu_1 = \sum_{i=k+1}^L i \Pr(i|c_1) = \sum_{i=k+1}^L \frac{ip_i}{\omega_1} = \frac{\mu_T - \mu(k)}{1 - \omega(k)} \quad (1.5)$$

where

$$\mu_T = \mu(L) = \sum_{i=1}^L ip_i \quad (1.6)$$

is the overall mean level of the original image.

The class variances are given by:

$$\sigma_0^2 = \sum_{i=1}^k (i - \mu_0)^2 \Pr(i|c_0) = \sum_{i=1}^k (i - \mu_0)^2 p_i / \omega_0 \quad (1.7)$$

$$\sigma_1^2 = \sum_{i=k+1}^L (i - \mu_1)^2 \Pr(i|c_1) = \sum_{i=k+1}^L (i - \mu_1)^2 p_i / \omega_1 \quad (1.8)$$

which require the calculation of second-order cumulative moments.

The proposed measure of optimality uses the following discriminant criterion measures, or measures of class separability:

$$\lambda = \sigma_B^2 / \sigma_W^2; \quad \kappa = \sigma_T^2 / \sigma_W^2; \quad \eta = \sigma_B^2 / \sigma_T^2 \quad (1.9)$$

where

$$\sigma_W^2 = \omega_0 \sigma_0^2 + \omega_1 \sigma_1^2 \quad (1.10)$$

$$\sigma_B^2 = \omega_0 (\mu_0 - \mu_T)^2 + \omega_1 (\mu_1 - \mu_T)^2 \quad (1.11)$$

$$\sigma_T^2 = \sum_{i=1}^L (i - \mu_T)^2 p_i \quad (1.12)$$

are the *within-class variance*, the *between-class variance*, and the *total variance of levels*, respectively. Notice that σ_T^2 is constant over the whole image, so the expense of its calculation can be disregarded.

Since σ_W^2 requires first- and second-order statistics, but σ_B^2 requires only first-order statistics, η is the simplest criterion to calculate.

The optimal threshold k^* that maximises η , or equivalently maximises the between-class variance σ_B^2 is selected by sequential search using the following derivations of the previous formulae:

$$\eta(k) = \sigma_B^2(k) / \sigma_T^2 \quad (1.13)$$

$$\sigma_B^2(k) = \frac{[\mu_T \omega(K) - \mu(k)]^2}{\omega(k)[1 - \omega(k)]} \quad (1.14)$$

As σ_T^2 is constant, the solution can be given as:

$$k^* \leftarrow \max_{1 \leq k < L} \sigma_B^2(k) \quad (1.15)$$

This solution provides a crisp threshold value which gives the best distinction between foreground and background pixels according to statistical analysis.

1.2.2 k -Means Clustering

Distinct from thresholding, clustering involves determining the classes themselves, rather than a threshold value between. In the most prominent clustering algorithm, k -means, each class is represented by a single value, called

the class centroid, which uniquely describes that class. The class centroid is calculated as the mean value of all members of the class.

Determining optimal clusters in k -means makes use of a recursive method to adjust the class centroids until they best represent what the algorithm determines are the clusters. Initially the centroids are placed arbitrarily, and the samples (image pixels) are classified according to the centroids using a distance-related function of membership. After this classification is complete, new class centroids are calculated based on the resultant clusters, and the process is repeated until the centroids don't move significantly between one iteration and the next. At this stage, we can say that the centroids (and thus the clusters) are optimal based on the initial configuration.

Given an image of N pixels ($x_j, \quad j = 1, \dots, N$), being partitioned into $c = 2$ classes ($G_i, \quad i = 1, \dots, c$), the algorithm minimises a dissimilarity (or distance) function:

$$J = \sum_{i=1}^c J_i = \sum_{i=1}^c \left(\sum_{k, x_k \in G_i} \|x_k - C_i\|^2 \right) \quad (1.16)$$

where C_i is the centroid of cluster i . That is, the sum of the distances of all pixels from their respective class centroids.

Algorithm:

1. The algorithm initially places the class centroids arbitrarily.
2. Then the membership of each pixel (j) in each class (i) is calculated using:

$$u_{ij} = \begin{cases} 1 & \text{if } \|x_j - C_i\|^2 \leq \|x_j - C_k\|^2, \quad \text{for each } k \neq i \\ 0 & \text{otherwise} \end{cases} \quad (1.17)$$

3. The objective function is calculated using (1.16), and compared to the value at the previous iteration.
4. If the improvement is below a set threshold (which is arbitrarily chosen beforehand), stop. Otherwise, calculate new class centroids using:

$$C_i = \frac{1}{|G_i|} \sum_{k, x_k \in G_i} x_k \quad (1.18)$$

and repeat from step 2.

Because every iteration of the algorithm improves on the previous configuration, the solution that it converges on is sub-optimal, dependant on the initial configuration. In order to approach a more global optimum, the procedure may be repeated several times using different initial configurations and the objective function is then minimised over all attempts; or more complicated dynamic programming techniques may be developed to predict better initial values for the centroids.

A common variation of k -means clustering, k -harmonic means (KHM) was proposed by Zhang et. al. in 1999-2000[20, 21] which alters the objective function to use the harmonic mean of the distance from each data point to all centroids.

The harmonic mean gives a low value for each data point when it is close to any one centroid. It is similar to the function used in k -means, but it is a smooth differentiable function.

The KHM technique has a fuzzy membership function (that is, pixels are assigned a degree of membership to every cluster, instead of absolute membership in a single cluster) which is distance-weighted to allow the centroids to spread to cover the data.

The KHM technique is similar in this respect to FCM (described below), but less popular in subsequent literature — more people have modified FCM. This document will describe the FCM technique in detail, providing a base of general knowledge for further research into KHM and other similar techniques.

1.2.3 Fuzzy *c*-Means Clustering

A fuzzy generalisation exists for k -means clustering, called fuzzy c -means, or FCM. FCM was proposed initially by Dunn in 1973[10] then improved upon by Bezdek in 1979[11]. The essential change it makes to the k -means algorithm is in the determination and expression of pixels' class memberships, from boolean membership to fuzzy; as a result the calculation of class means has to be modified to incorporate each pixel's fuzzy membership in both classes.

Algorithm:

1. To fuzzify k -means into FCM, the initialisation arbitrarily assigns class memberships of each pixel, rather than the values of the class centroids themselves. The initial memberships are constrained by:

$$\sum_{i=1}^c u_{ij} = 1, \forall j = 1, \dots, N \quad (1.19)$$

2. Class centroids are calculated using:

$$C_i = \frac{\sum_{j=1}^n u_{ij}^m x_j}{\sum_{j=1}^n u_{ij}^m} \quad (1.20)$$

where C_i is the centroid of cluster i , the membership u_{ij} is between 0 and 1, and m is an arbitrary weighting exponent, $1 < m < \infty$. A large

value for m will dramatically decrease the effect of low-membership pixels on the calculated centroid.

3. The objective function is altered to accommodate fuzzy memberships, and calculated as the dissimilarity between the class centroids and the data points thus:

$$J(U, C_1, \dots, C_c) = \sum_{i=1}^c J_i = \sum_{i=1}^c \sum_{j=1}^n u_{ij}^m d_{ij}^2 \quad (1.21)$$

where d_{ij} is the difference between the i^{th} centroid and the j^{th} pixel.

4. If the improvement over the previous iteration is below a threshold, stop. Otherwise, calculate new memberships for all pixels using:

$$u_{ij} = \frac{1}{\sum_{k=1}^c \left(\frac{d_{ij}}{d_{kj}} \right)^{\frac{1}{m-1}}} \quad (1.22)$$

and repeat from step 2.

The more complicated calculations allow for more accurate classifications at every stage of the algorithm, including degrees of membership which reduce the effect of less-clearly-defined pixels, and can also be used as a degree of confidence (or inherent error) in the resulting classification. However, as with all k -means algorithms, the solution is sub-optimal, depending on the initial configuration.

Many adaptations of the FCM clustering method have been proposed to improve its performance in specialised situations. For example, by injecting a term into the objective function that constrains the membership function with its neighbourhood, Lei Jiang and Wenhui Yang were able to compensate for noise and intensity inhomogeneities in Magnetic Resonance (MR) images[12].

Similarly Dao-Qiang Zhang and Song-Can Chen modified the objective function using a kernel-induced distance metric, instead of the Euclidean distance, and a spatial penalty on the membership functions to further improve segmentation in the presence of noise, intensity inhomogeneities and other artefacts common in MR images[13].

This document provides a description of the standard fuzzy c -means algorithm to the point that the reader should be confident in approaching these and similarly adapted techniques. However the techniques themselves will not be described.

1.3 Shortcomings of Otsu, k -Means and Fuzzy

c -Means for Image Segmentation

Known thresholding and clustering techniques, such as Otsu’s threshold and fuzzy c -means, have shown high levels of popularity in the past thirty years, and are very simple algorithms to implement that run quickly compared to other, more complicated procedures. However, these techniques use only intensity data to perform segmentations, and as such don’t take into account the spatial structure of the image. By such reasoning, all three images in Figure 1.1 are identical, in that they have identical histograms, with the same mean and deviances. The omission of spatial data will not take into account the full information available in the image data, as an image without spatial structure is no longer an image — rather, it becomes a simple set of values, and is of little practical use to an observer.

Additionally, the classic techniques above, while accurate when segmenting ‘ideal’ images (with distinct classes and an absence of noise and blurring),

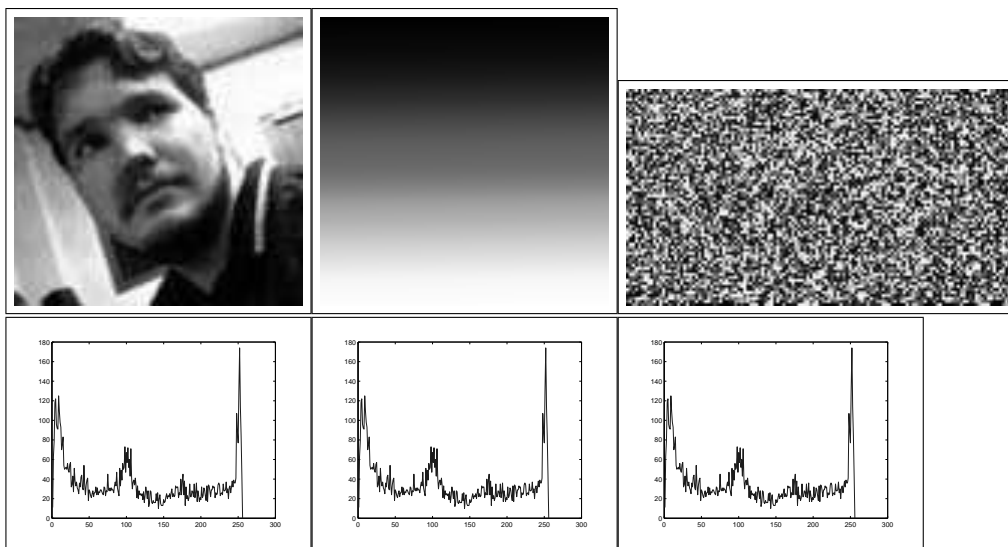


Figure 1.1: Three different images with identical histograms.

tend to fall down when applied to images with such imperfections, as evidenced in Chapter 4.

Other image segmentation techniques, for example region growing [29, pg. 612-617], use the image’s structure to perform segmentation. This technique improves results for imperfect images at the cost of either complex algorithms and slow calculations, or requiring human intervention, or both, ultimately slowing down the segmentation and decreasing its effectiveness in a real-world situation.

It could be said that an ideal solution to image segmentation is one that is accurate in imperfect conditions, reasonably fast, and incorporates the image’s spatial structure in the calculation, with minimal input from a user.

A novel technique, segmentation by morphological watersheds[29, pp. 617-626], attempts to present a solution to image segmentation by visualising the problem in the context of a completely different field of research — en-

vironmental geography. Despite obvious difficulties apparent in watershed segmentation[29, pg. 624], the idea of borrowing techniques from different fields of research may prove beneficial when attempting to devise better image segmentation techniques.

Chapter 2

Geostatistical Threshold

An attempt is given to provide an improved solution to the problem of image segmentation. By combining a technique used in geological studies, namely geostatistics, an approach is designed that replaces the histogram-based statistical analysis of Otsu's threshold with a spatial statistical analysis.

2.1 Geostatistics

Based on early work by South African geologists Krige, Sichel and de Wijs, Georges Matheron[22] proposed a new theory of regionalised variables — that is, variables that are distributed in space — in 1962, commonly known as geostatistics[23]. Simply put, geostatistics is the statistics of spatially correlated data. Particularly, it applies the theories of stochastic processes and statistical inference to geographic (spatial) occurrences. As such, it provides a means of analysing the spatial features of an image in the framework provided by Otsu's threshold.

The underlying concept of geostatistics is scales of spatial variance. Spatially independent data show uniform variance irrespective of the locations of the samples. However real-world spatial data will typically not be spatially independent. Samples taken close together tend to have more in common, or lower variance, than samples which are spaced at a greater distance. The function of variability and distance between samples is called semivariance.

In geostatistics three functions are used to describe the spatial correlation of samples: the correlogram, the covariance, and the semivariogram. An experimental semivariogram is an empirical estimate of the covariance of a Gaussian process, computed by measuring the mean-squared difference (*semivariance*) between two samples at points x and $x + h$. The semivariogram is the plot of semivariance over the distance h , known as the *lag*.

2.2 Experimental Semivariogram

A semivariogram is a graph of semivariance over distance between samples. As such, it can be useful in analysing the spatial structure of images, by comparing pixels to their neighbourhoods. If all pixels show low variance from their immediate neighbourhoods, the image is regionally homogenous, without high-contrast boundaries or edges.

Calculation of the semivariogram typically depends on prior knowledge of the correlation function of a sample. In terms of image processing, where pixel values may be considered arbitrary real-world samples without a clearly defined or calculable correlation function, simpler approximations are required.

The process of calculating an experimental semivariogram involves iterating over lag distances, and calculating the mean semivariance of every

pixel-relationship for each lag distance. The graph of semivariance over lag distance gives an experimental semivariogram.

Generally, the experimental semivariogram, $\gamma(h)$, of N samples is expressed as:[23, 25]

$$\gamma(h) = \frac{1}{2(N-h)} \sum_{i=1}^{N-h} [g(i+h) - g(i)]^2 \quad (2.1)$$

where $g(i)$ is the sample value at position i , and h is the lag distance.

For image processing, where the data set is a two dimensional array of pixels, the experimental semivariogram can be given as:[26]

$$\begin{aligned} \gamma(h) = \frac{1}{2} \left(\frac{1}{N_r N_c} \sum_{x=1}^{N_c} \sum_{y=1}^{N_r} [I(x+h, y) - I(x, y)]^2 \right. \\ \left. + \frac{1}{N_r N_c} \sum_{x=1}^{N_c} \sum_{y=1}^{N_r} [I(x, y+h) - I(x, y)]^2 \right) \quad (2.2) \end{aligned}$$

where $I(\cdot)$ is the pixel value at a given position, N_r and N_c are the number of rows and columns of the image, respectively, and h is the lag distance expressed in pixels.

Typically, the resulting graph of $\gamma(h)$ over h will approximate a logarithmic curve, as adjacent pixels in an image tend to have more in common with their immediate neighbours (lower variance at small lag distances), and less in common with distant pixels (higher variance at great lag distances), until they reach a “horizon” distance beyond which there is essentially no relationship between the pixels, at which point the semivariance graph should ideally plateau. In practice, however, one will typically find that after reaching a plateau the graph will again decrease, as at extreme lag distances the compared pixels will tend to have more in common, as they will be members of the same class — the background. As such it is practical to determine an

upper limit for the lag distance specific to the image. An ideal upper lag distance is one that does not exceed the size of any features in the image, that way the algorithm will not overlook a feature by comparing pixels spanning either side of it.

2.3 Geostatistical Threshold

As in Otsu’s method, a threshold can be evaluated by the variance of its resulting classes. We can say that the threshold resulting in the lowest sum of within-class variances is an optimal threshold.

Given that an image of N pixels and L intensity levels is divided at a threshold k into two classes c_1 and c_2 , such that c_1 denotes pixels with levels $[1, \dots, k]$, and c_2 denotes pixels with levels $[k + 1, \dots, L]$, where c_1 has N_1 pixels and c_2 has N_2 pixels ($N_1 + N_2 = N$), the variance of the threshold given in terms of geostatistics is:[28]

$$V(k, h) = N_1\gamma_1(k, h) + N_2\gamma_2(k, h) \quad (2.3)$$

where $\gamma_1(k, h)$ and $\gamma_2(k, h)$ are the class semivariances for a threshold at k and a lag distance of h .

The effect of the threshold is that one is essentially evaluating two images: one composed entirely of foreground pixels, and one of background. If both sub-images display low variance, the threshold is good according to our criteria. To this end, the semivariogram $\gamma(h)$ is calculated twice, once for each sub-image, and the two graphs are added together to give the overall variance for that threshold. This is achieved by initially flagging all pixels in the foreground class as ‘on,’ and all other pixels as ‘off,’ and calculating the semivariogram with the condition that all $I(\cdot)$ must be ‘on,’ otherwise

that iteration of the summation is impotent. In this way, the semivariance is only calculated between pixels of the same class. After the calculation, the pixels are toggled so that ‘off’ become ‘on’ and *vice-versa*, and the second semivariogram is calculated. The experimental semivariogram tolerates the resulting ‘dark spots’ of ‘off’ pixels in the images because this simply emulates the unevenly spaced geological samples for which the algorithm was originally designed.

The mean variance of a threshold up to a maximum lag distance n is calculated as:

$$\bar{V}(k) = \frac{1}{n} \sum_{h=1}^n V(k, h) \quad (2.4)$$

The optimal threshold k^* is the threshold that gives lowest mean variance. That is:

$$k^* \leftarrow \min_{1 \leq k < L} \bar{V}(k) \quad (2.5)$$

Chapter 3

Experiments

3.1 Images

The images used in this project will fall under many broad categories, to illustrate the advantages and disadvantages of the different segmentation techniques in various contexts. For the most part images related to bioinformatics will be analysed, as a study of available literature suggests that the primary impacting uses of image processing techniques are in bioinformatics study areas. Bioinformatics images will include those used to study cell growth and structure, analyse the effects of treatments on cell populations, and to diagnose diabetic retinopathy from retinal photographs. Additionally images of interest from non-bioinformatics areas will be included, which may be useful in other artificial intelligence and image recognition applications.

3.2 Techniques

To demonstrate the geostatistical threshold technique, two segmentations will be calculated: one using a single-pixel lag distance ($h = 1$), and another with the mean of lag distances up to 3 pixels ($h = 1, \dots, 3$) in both the horizontal and vertical directions. This range has been determined through experimentation to show consistent results across a wide range of images.

Due to the wide variety of applications of image segmentations, comparison of techniques in any meaningful way is difficult. A judgement can be made subjectively, typically by an expert in the field for which the segmentation is taking place. For example, to determine which technique best segments images of cancer cells for analysis of size and shape information, the evaluation of the techniques would be best performed by the pharmacologist who will be analysing the results.

In practical applications, criteria determining optimality may vary widely. For example, when using image segmentation to determine populations of cells, where cells in the image may be touching or overlapping, the best segmentation algorithm may be one which provides clear distinction between the cells, rather than attempting to maintain their original size. For that reason, all images displayed below will be evaluated according to specific subjective criteria that may apply to each particular image.

In order to compare FCM with other non-fuzzy segmentation techniques, we are required to determine crisp memberships for all pixels. The most logical way to achieve this is to assign each pixel full membership in the class

it mostly strongly represents.

$$u_{ij} = \begin{cases} 1 & \text{if } u_{ij} \geq 0.5 \\ 0 & \text{otherwise} \end{cases} \quad (3.1)$$

Additionally, it is possible to represent k -means and de-fuzzified FCM segmented images by a single threshold value which well represents the segmentation. This threshold is calculated as the minimum value of pixels in the original image that were eventually assigned to the ‘white’ class. As k -means and FCM base their calculations entirely on the intensity value of the pixels, and the resulting classes are linearly separable, all ‘white’ pixels will always be lighter than all ‘black’ pixels, so this artificial threshold accurately describes and can recreate the segmentation.

Finally, it should be noted that retinal photograph images require extra processing, as the images themselves actually comprise three classes: darker foreground objects, lighter background, and a black border, illustrated in Figure **3.1**. As the border consistently displays certain properties — such as: very dark, found in the corners of images — it is trivial to remove those pixels from consideration when performing segmentation. Results given below have had border pixels removed prior to feature segmentation.

For illustrative purposes, border pixels in retinal images have been classified as “foreground” because, being dark, they have more in common with foreground pixels than background, and in the case of thresholding, will always be darker than the threshold, along with the foreground.

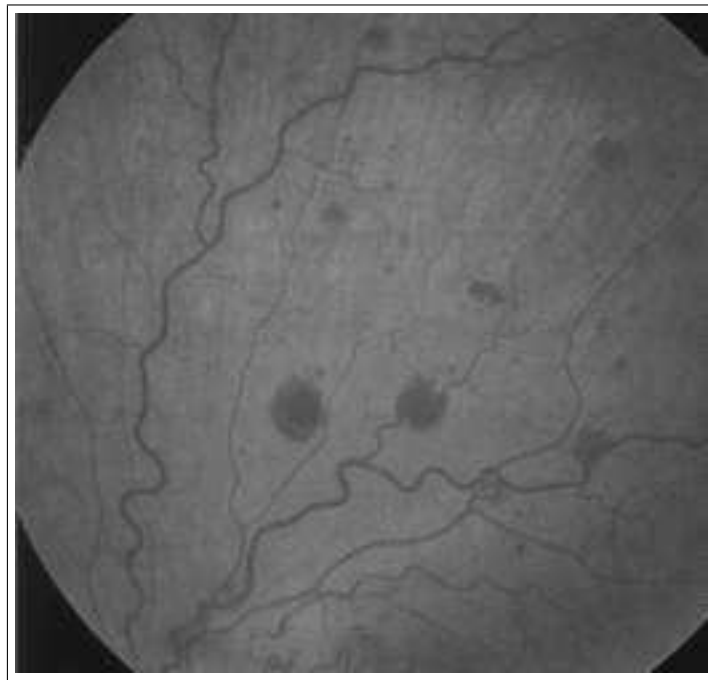


Figure 3.1: Retinal image showing dark features on a light background, with black border pixels in the corners of the image.

Chapter 4

Results and Discussions

Result data are displayed in tabular form in Table 4.1, and typical image results are illustrated. These displayed images have been found by the author to demonstrate typical behaviour of the segmentation techniques detailed above in various situations.

In a simple image such as Figure 4.1, with a clearly bimodal histogram, crisp (non-blurry) features, and no noise, all techniques performed very well, choosing thresholds very similar to each other (within 5 levels — 1.95% of the overall range of levels). In such a case, the best technique to use would be the one that is fastest to run or simplest to implement.

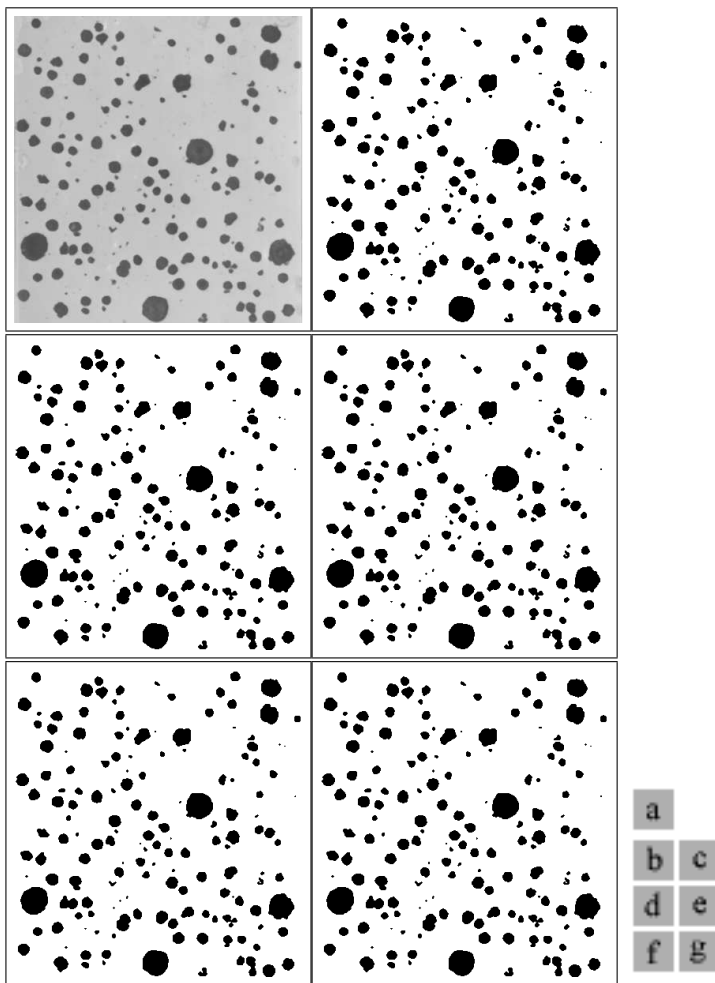
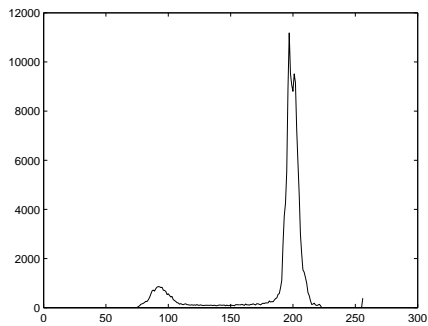


Figure 4.1: Nodules. “nodules1.tif” (a) image histogram, (b) original image, (c) Otsu, (d) k -means, (e) FCM, (f) Geostatistical ($h = 1$), (g) Geostatistical (mean of $h = 1, 2$, and 3)

Figures 4.2 to 4.28 compare results of non-spatial and spatial techniques and in more complex images; in the presence of staining, poorly-defined blurry features, and noise. It is clear that FCM is particularly sensitive to noise, for example in Figure 4.7.

Figures 4.7 and 4.13 show in finer detail regions where the effect of staining and blurriness has caused Otsu's threshold and k -means to poorly segment the image. Cells are much better defined and clearly distinguished in those segmentations produced by geostatistical thresholding.

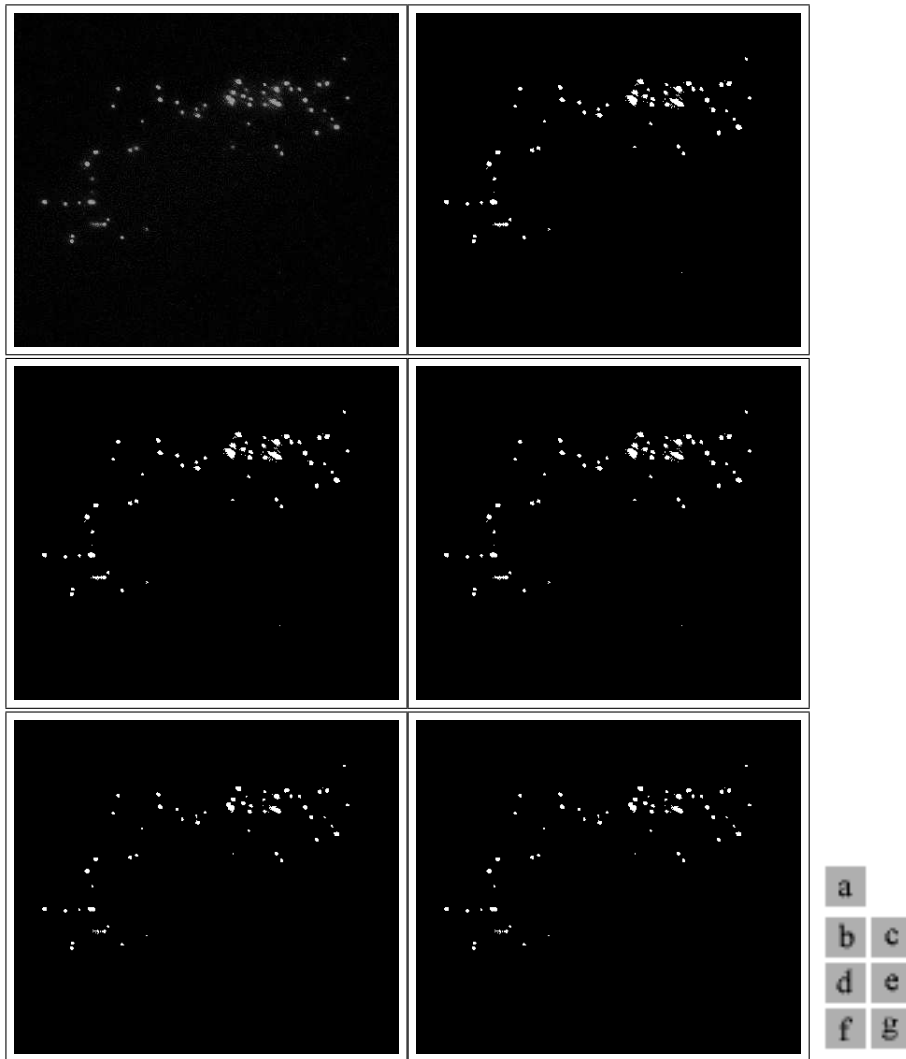
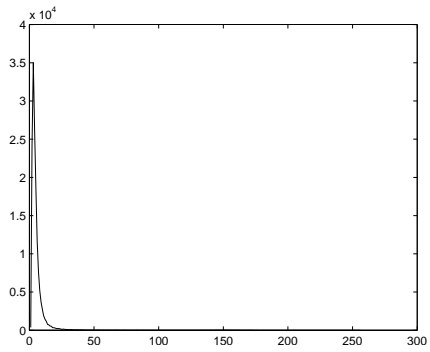


Figure 4.2: Fluorescence Cells. “imageA.jpg” (a) image histogram, (b) original image, (c) Otsu, (d) k -means, (e) FCM, (f) Geostatistical ($h = 1$), (g) Geostatistical (mean of $h = 1, 2, \text{ and } 3$)

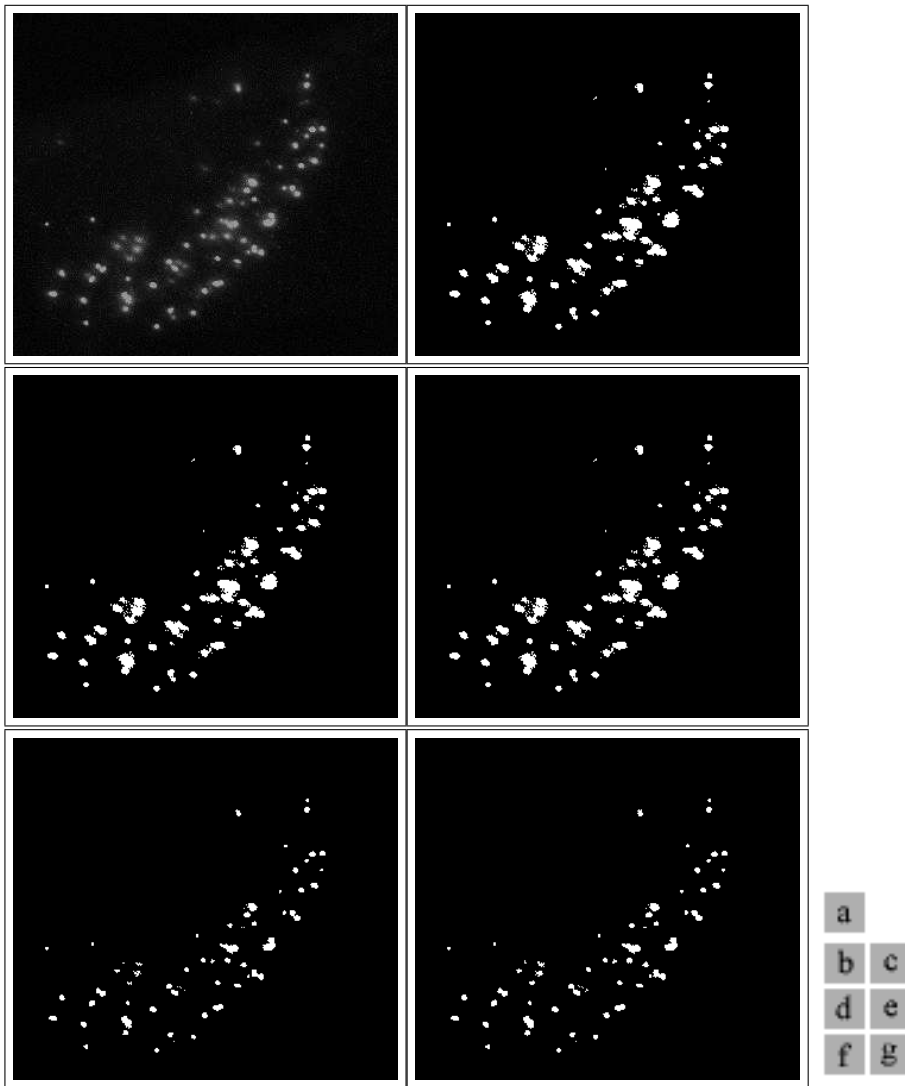
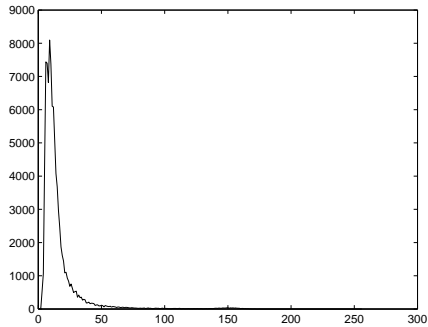


Figure 4.3: Fluorescence Cells. “imageB.jpg” (a) image histogram, (b) original image, (c) Otsu, (d) k -means, (e) FCM, (f) Geostatistical ($h = 1$), (g) Geostatistical (mean of $h = 1, 2$, and 3)

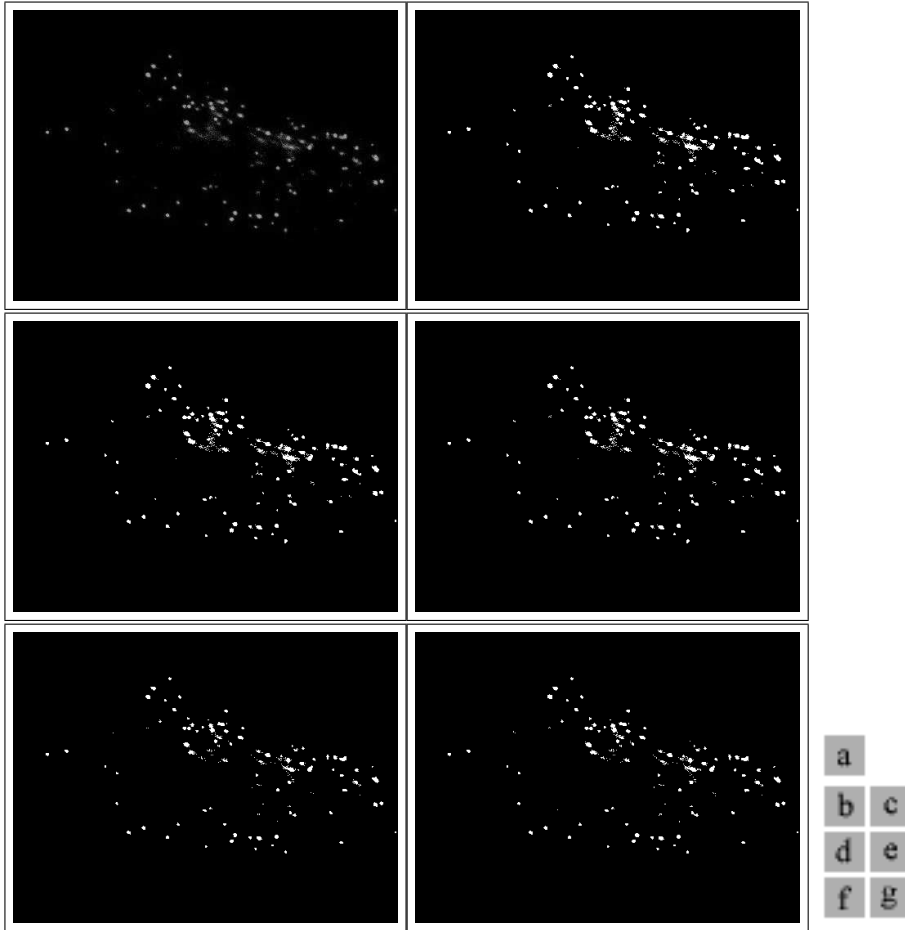
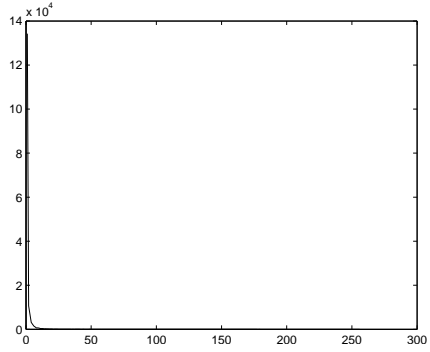


Figure 4.4: Fluorescence Cells. “imageC.jpg” (a) image histogram, (b) original image, (c) Otsu, (d) k -means, (e) FCM, (f) Geostatistical ($h = 1$), (g) Geostatistical (mean of $h = 1, 2$, and 3)

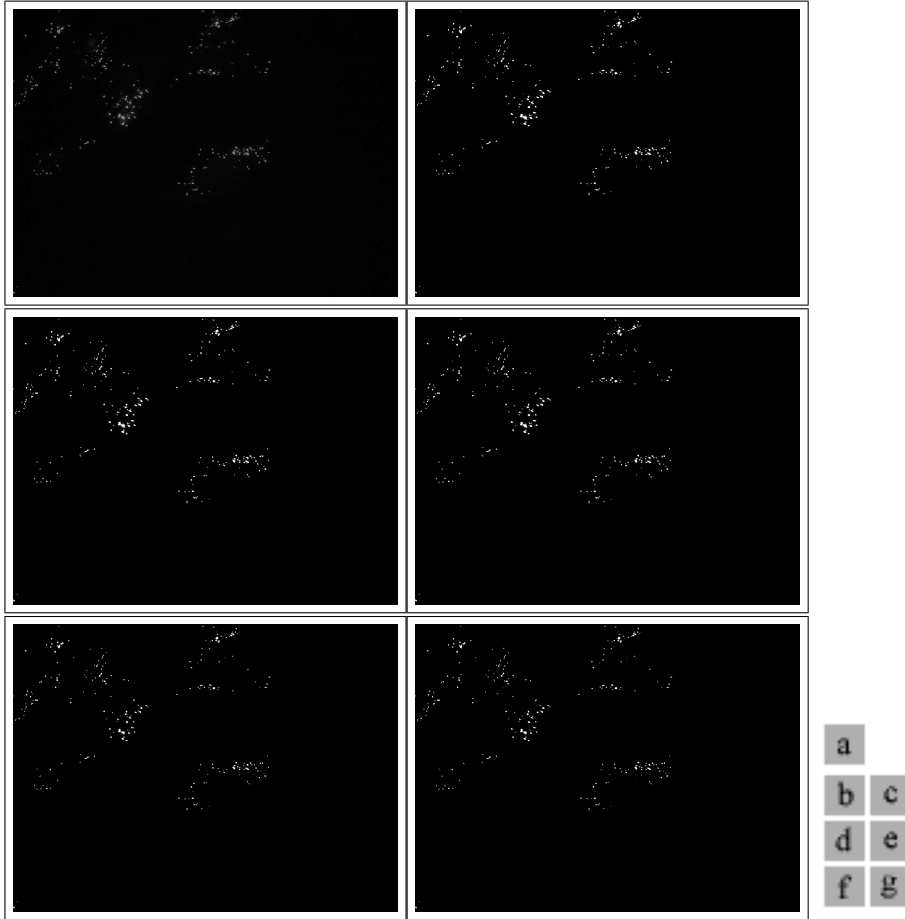
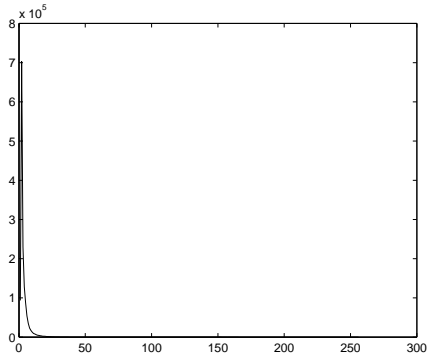


Figure 4.5: Fluorescence Cells. “imageD.jpg” (a) image histogram, (b) original image, (c) Otsu, (d) k -means, (e) FCM, (f) Geostatistical ($h = 1$), (g) Geostatistical (mean of $h = 1, 2$, and 3)

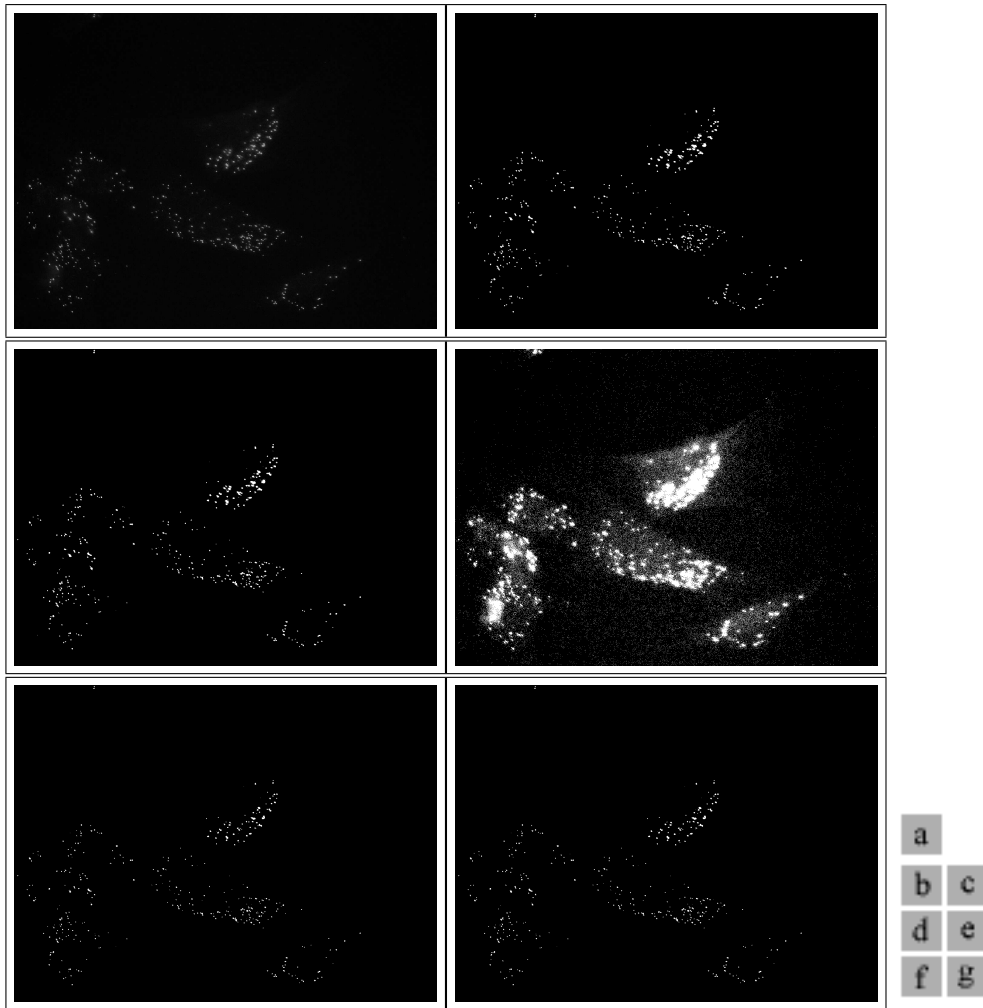
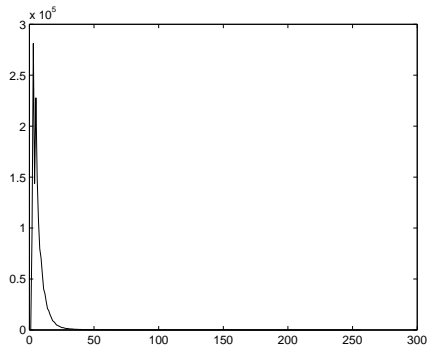


Figure 4.6: Fluorescence Cells. “imageE.jpg” (a) image histogram, (b) original image, (c) Otsu, (d) k -means, (e) FCM, (f) Geostatistical ($h = 1$), (g) Geostatistical (mean of $h = 1, 2$, and 3)

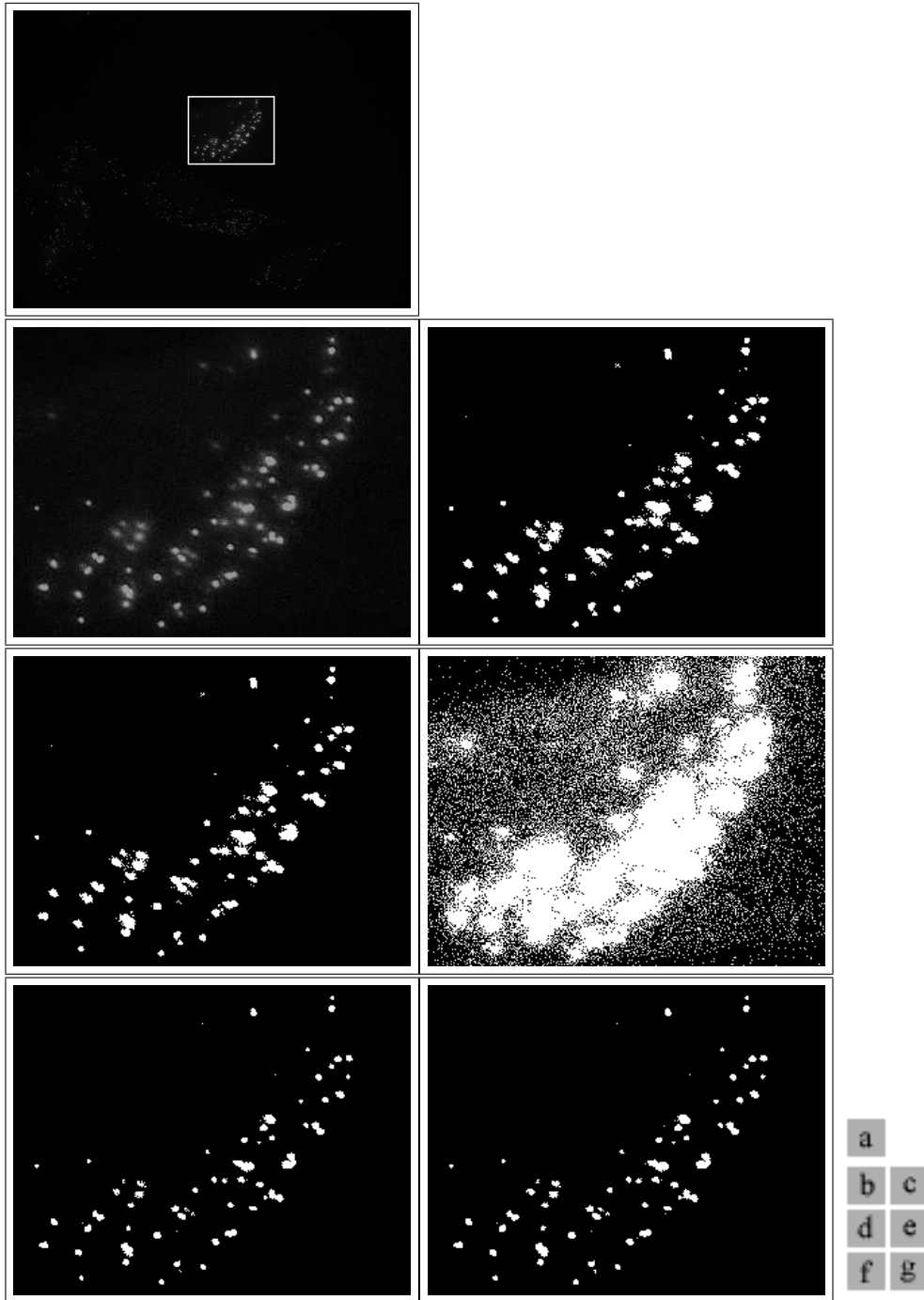


Figure 4.7: Fluorescence Cells (Detail). Detail of “imageE.jpg” (a) original image with detail region marked, (b) original image detail, (c) Otsu, (d) k -means, (e) FCM, (f) Geostatistical ($h = 1$), (g) Geostatistical (mean of $h = 1, 2, \text{ and } 3$)

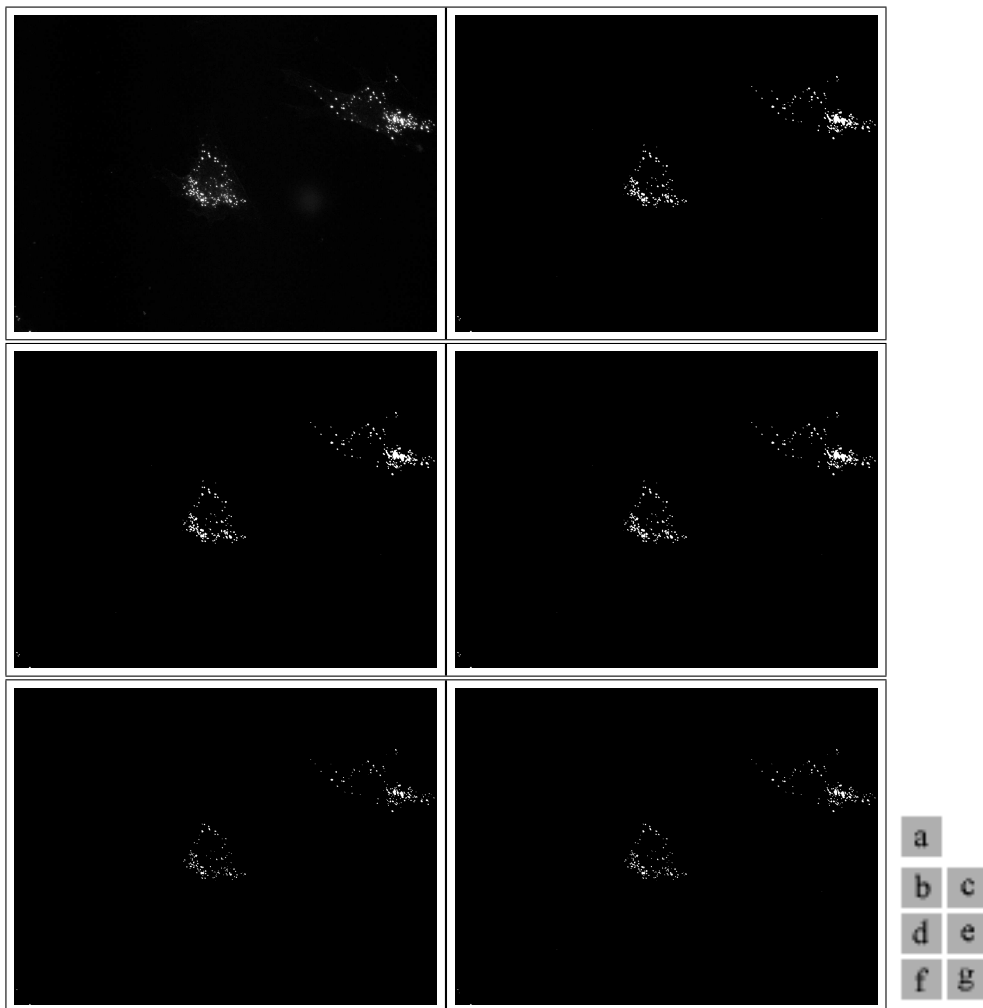
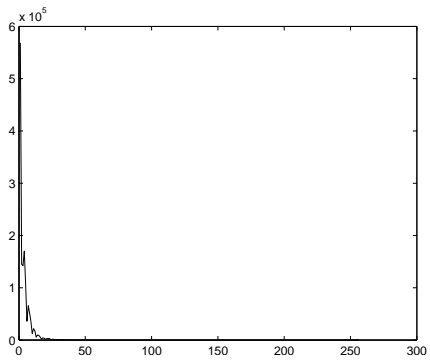


Figure 4.8: Cell Clusters. “px1.jpg” (a) image histogram, (b) original image, (c) Otsu, (d) k -means, (e) FCM, (f) Geostatistical ($h = 1$), (g) Geostatistical (mean of $h = 1, 2$, and 3)

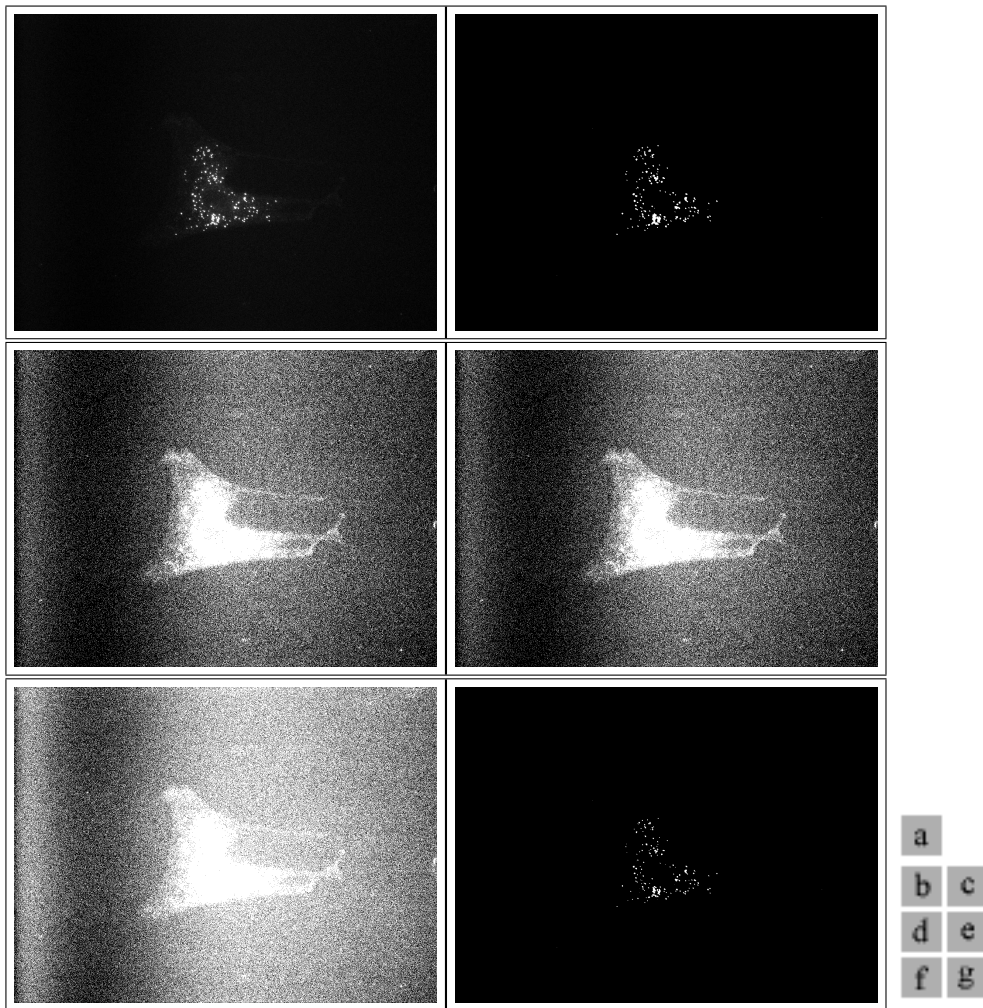
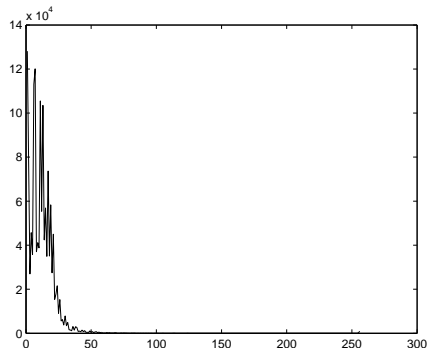


Figure 4.9: Cell Clusters. “px2.jpg” (a) image histogram, (b) original image, (c) Otsu, (d) k -means, (e) FCM, (f) Geostatistical ($h = 1$), (g) Geostatistical (mean of $h = 1, 2, \text{ and } 3$)

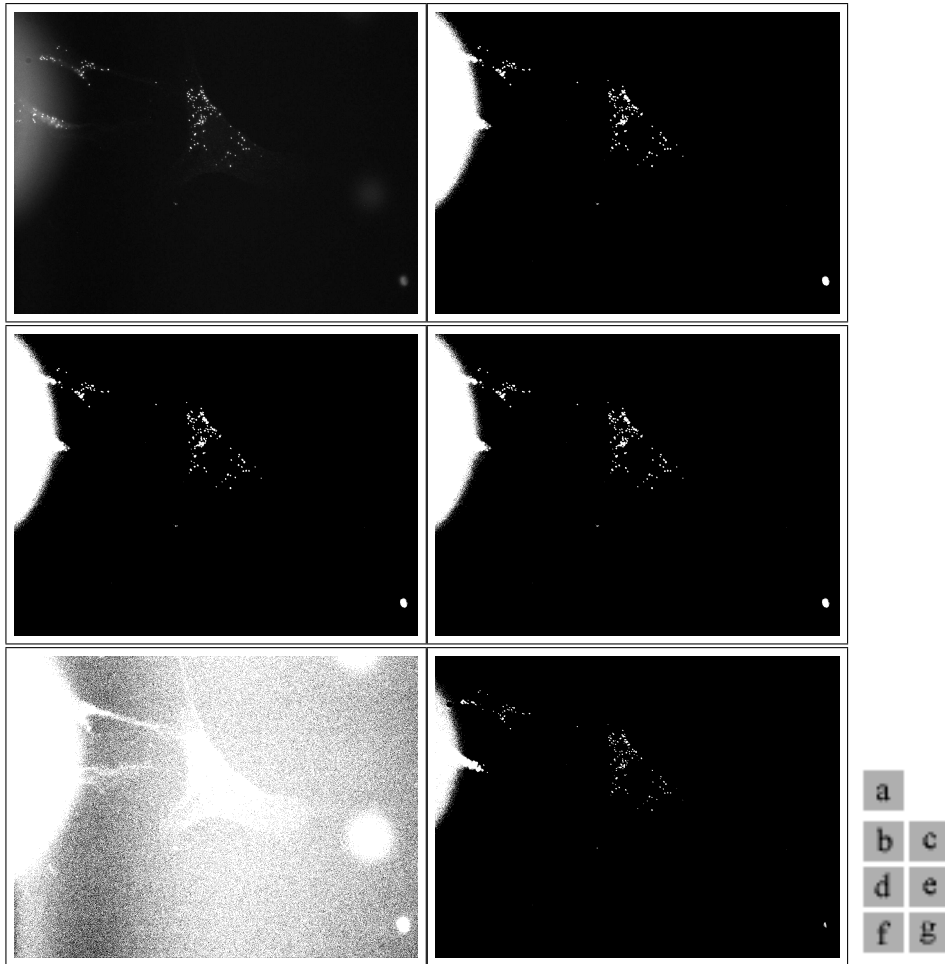
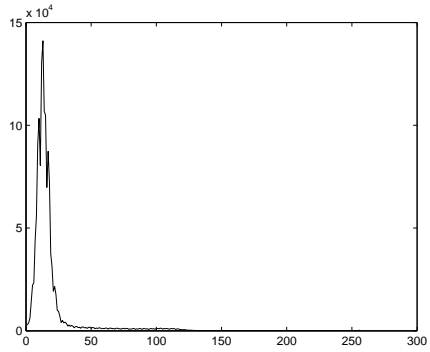


Figure 4.10: Cell Clusters. “px3.jpg” (a) image histogram, (b) original image, (c) Otsu, (d) k -means, (e) FCM, (f) Geostatistical ($h = 1$), (g) Geostatistical (mean of $h = 1, 2$, and 3)

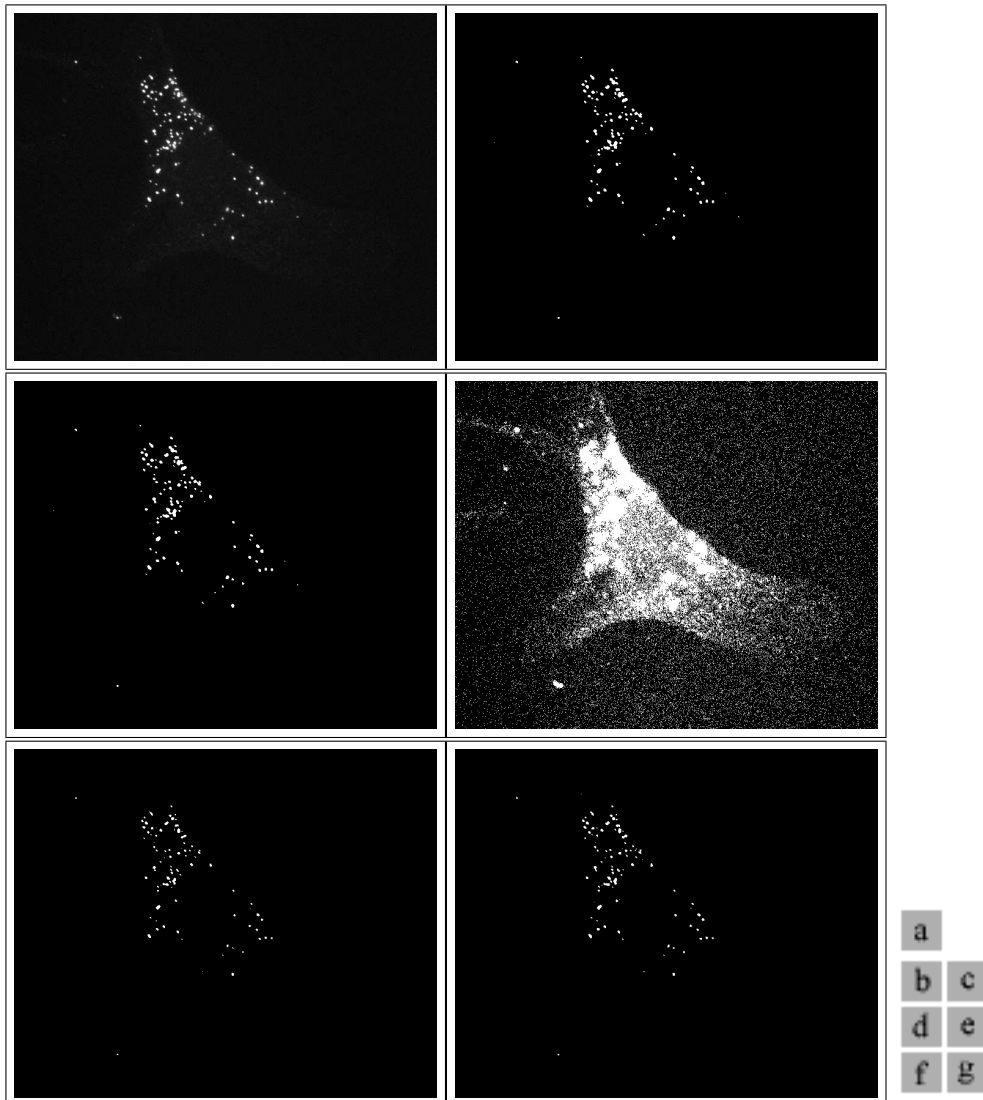
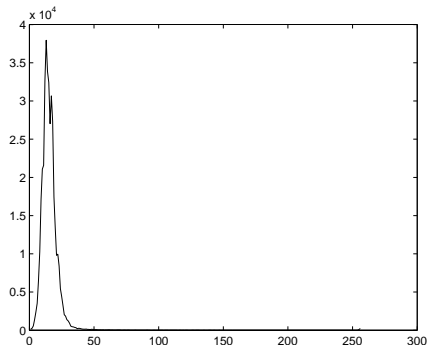


Figure 4.11: Cell Clusters. “px3.jpg” manually cropped to a region of interest before segmentation. (a) image histogram, (b) original image, (c) Otsu, (d) k -means, (e) FCM, (f) Geostatistical ($h = 1$), (g) Geostatistical (mean of $h = 1, 2$, and 3)

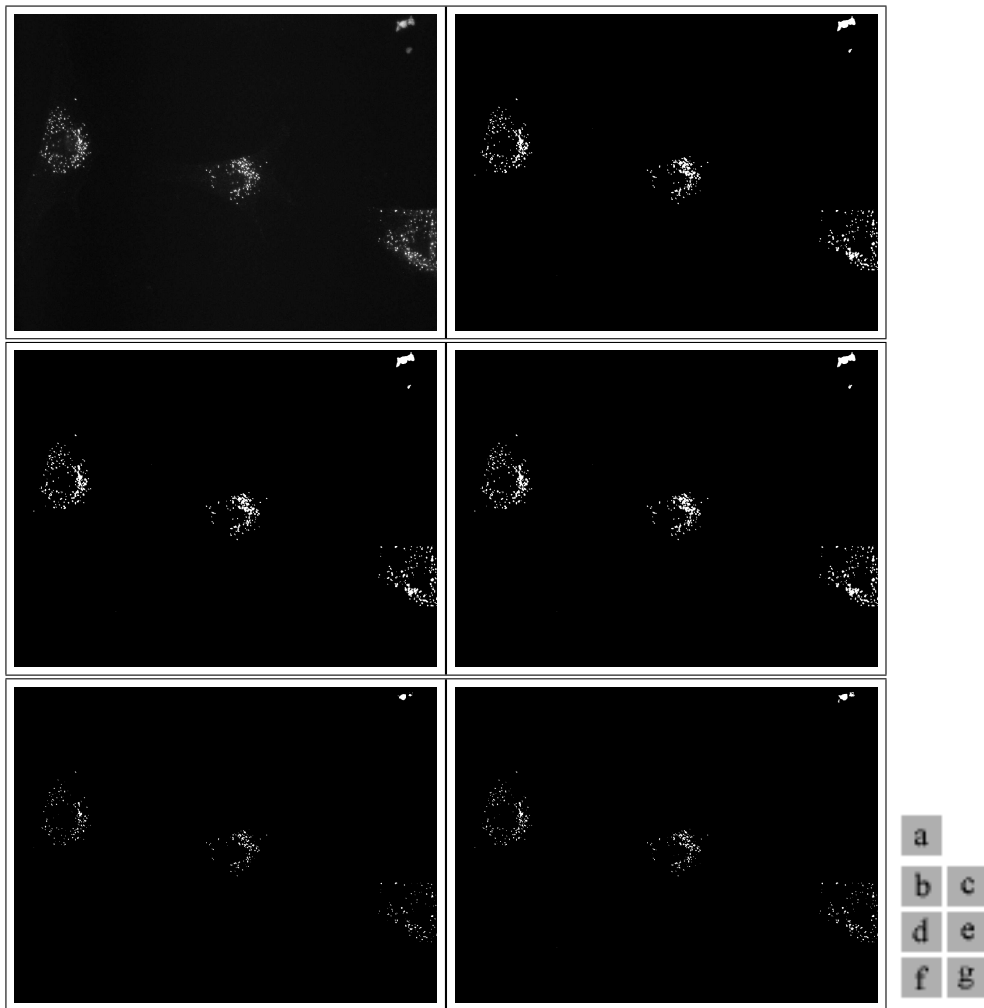
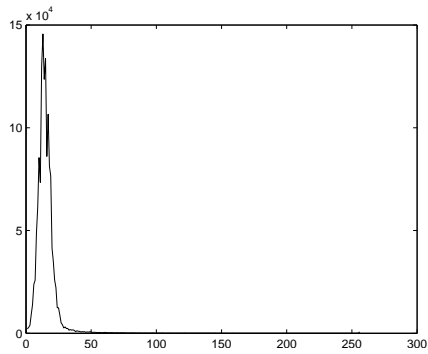


Figure 4.12: Cell Clusters. “px4.jpg” (a) image histogram, (b) original image, (c) Otsu, (d) k -means, (e) FCM, (f) Geostatistical ($h = 1$), (g) Geostatistical (mean of $h = 1, 2$, and 3)

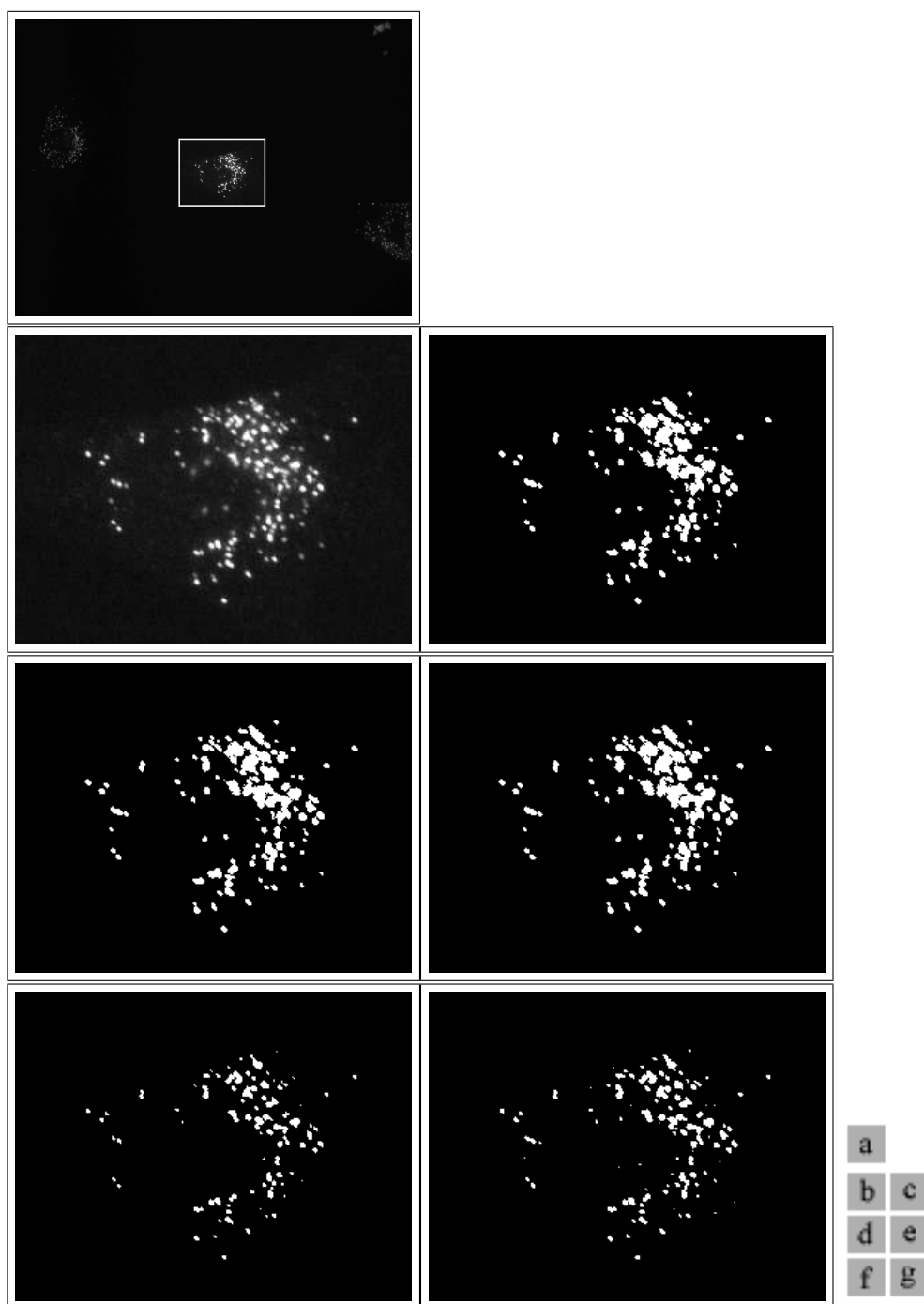


Figure 4.13: Cell Clusters (Detail). Detail of “px4.jpg” (a) original image with detail region marked, (b) original image detail, (c) Otsu, (d) k -means, (e) FCM, (f) Geostatistical ($h = 1$), (g) Geostatistical (mean of $h = 1, 2$, and 3)

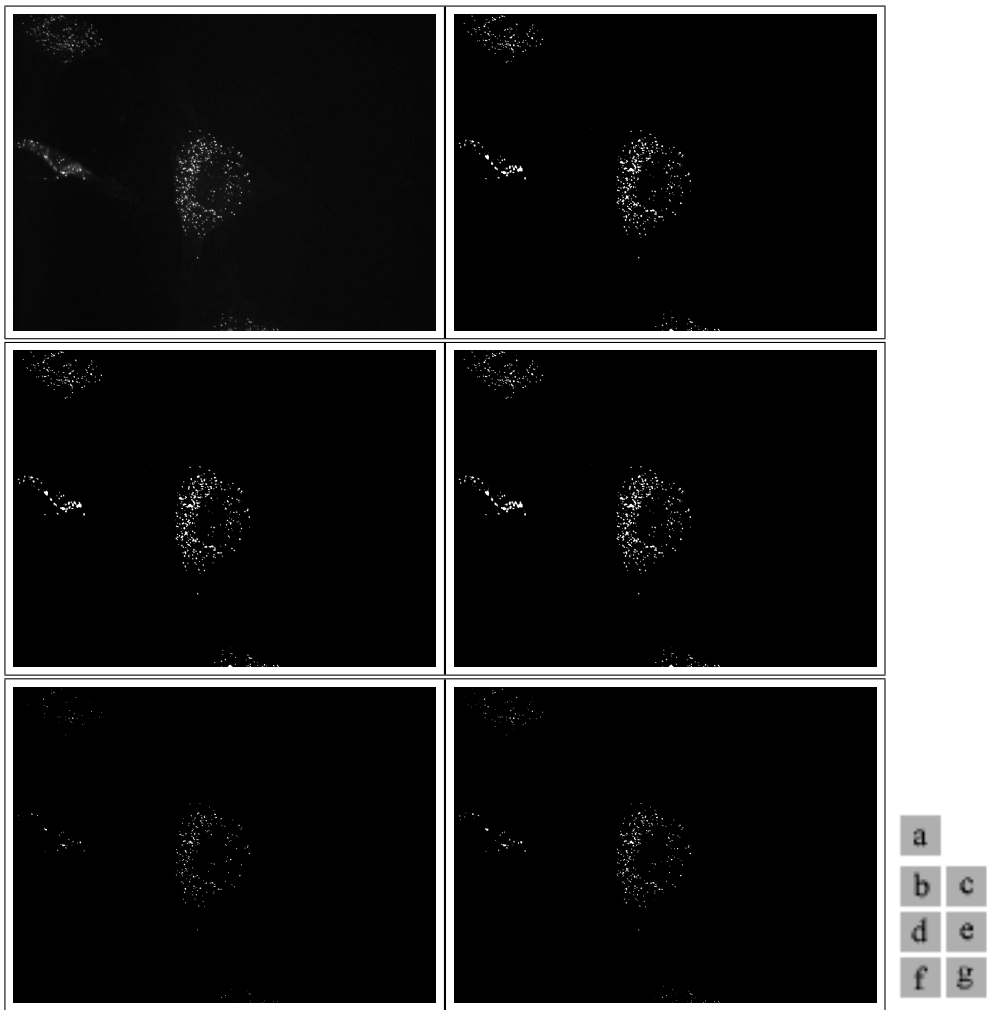
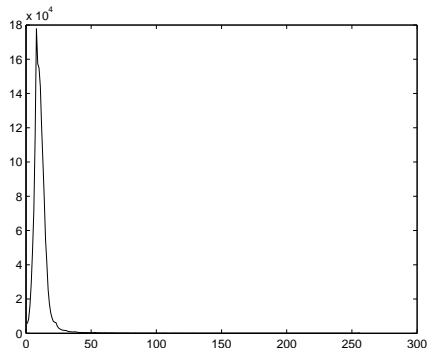


Figure 4.14: Cell Clusters. “px5.jpg” (a) image histogram, (b) original image, (c) Otsu, (d) k -means, (e) FCM, (f) Geostatistical ($h = 1$), (g) Geostatistical (mean of $h = 1, 2$, and 3)

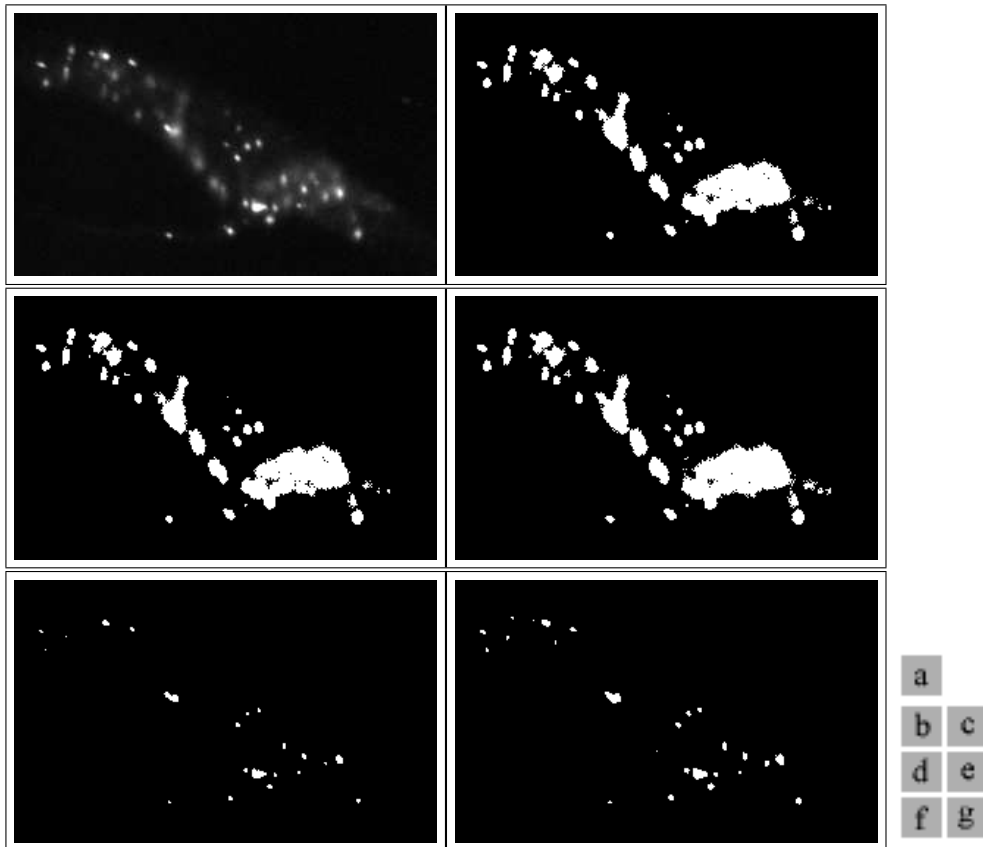
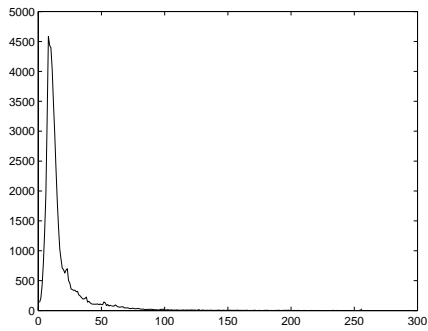


Figure 4.15: Cell Clusters. “px5.jpg” manually cropped to a region of interest before segmentation. (a) image histogram, (b) original image, (c) Otsu, (d) k -means, (e) FCM, (f) Geostatistical ($h = 1$), (g) Geostatistical (mean of $h = 1, 2$, and 3)

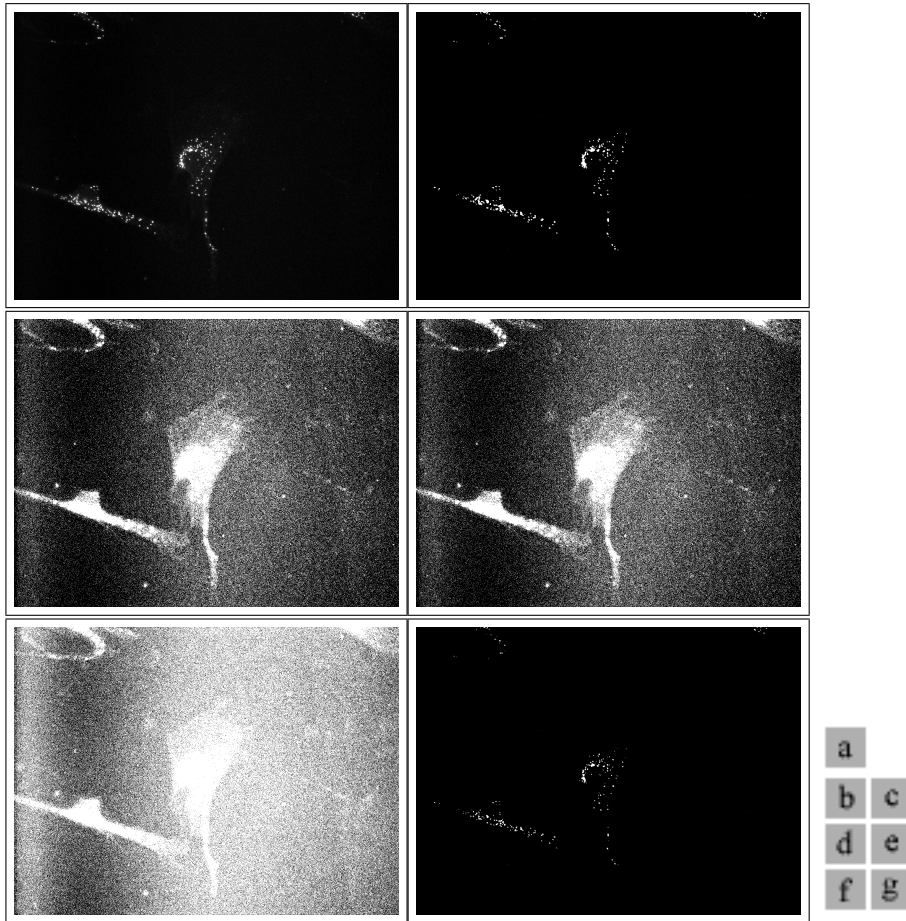
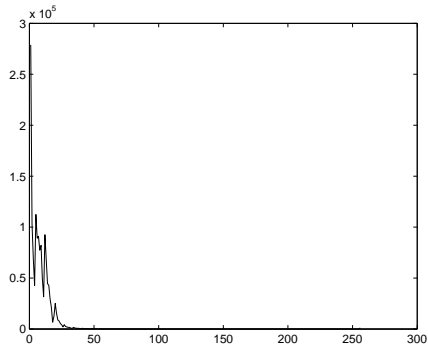


Figure 4.16: Cell Clusters. “px6.jpg” (a) image histogram, (b) original image, (c) Otsu, (d) k -means, (e) FCM, (f) Geostatistical ($h = 1$), (g) Geostatistical (mean of $h = 1, 2, \text{ and } 3$)

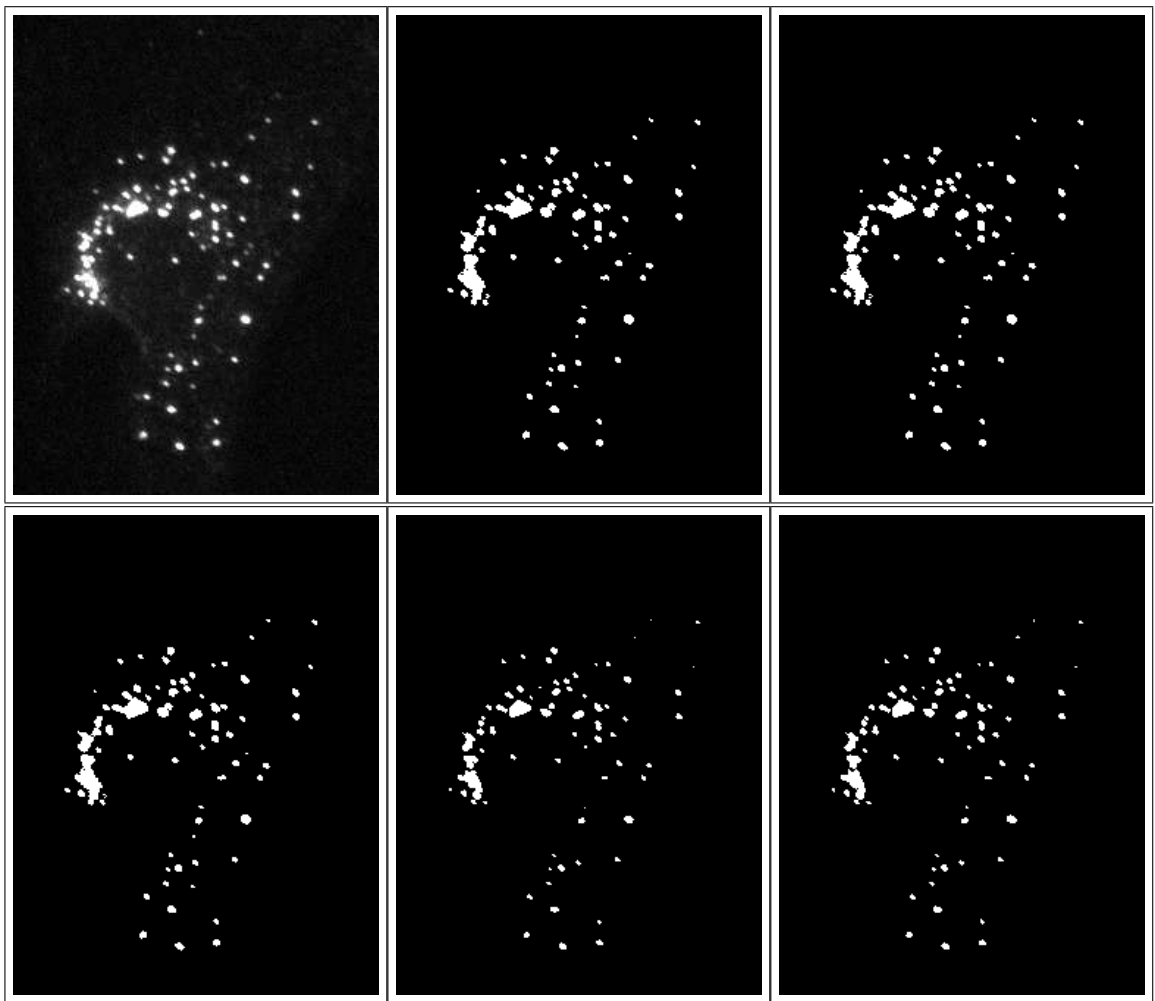
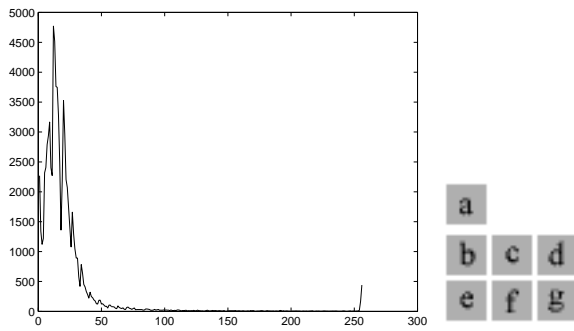


Figure 4.17: Cell Clusters. “px6.jpg” manually cropped to a region of interest before segmentation. (a) image histogram, (b) original image, (c) Otsu, (d) k -means, (e) FCM, (f) Geostatistical ($h = 1$), (g) Geostatistical (mean of $h = 1, 2$, and 3)

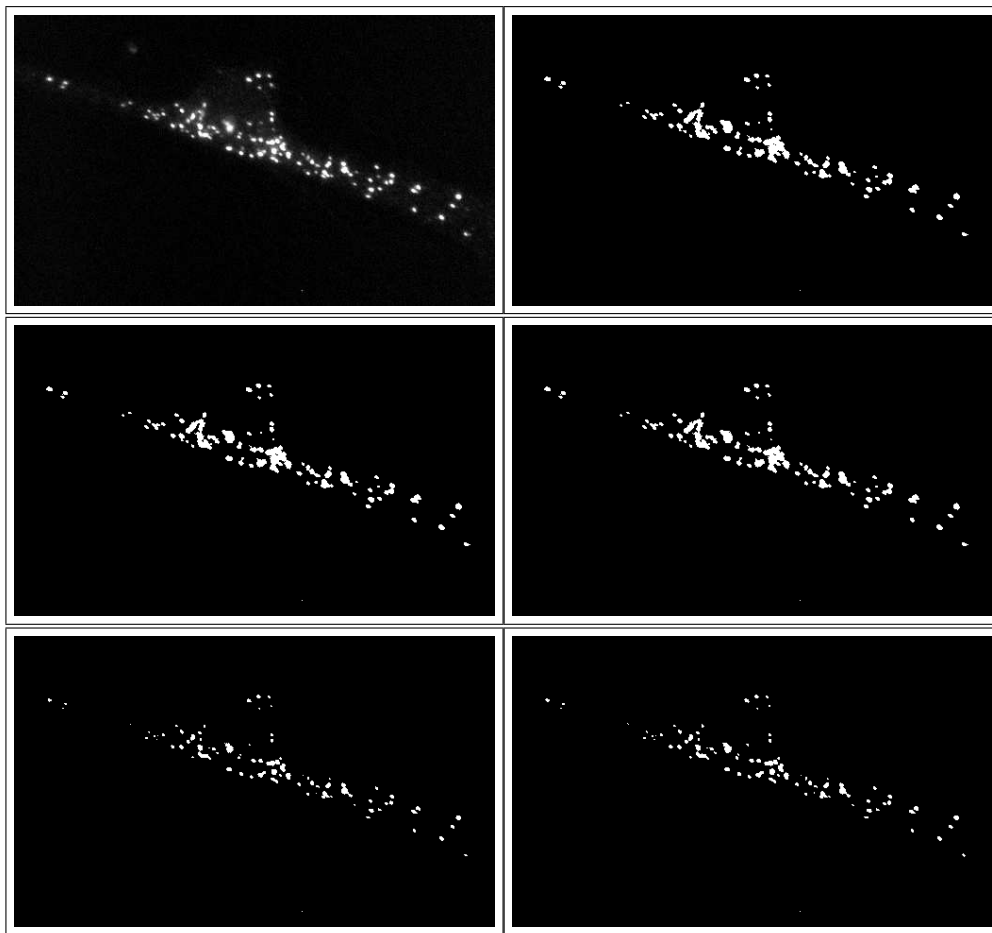
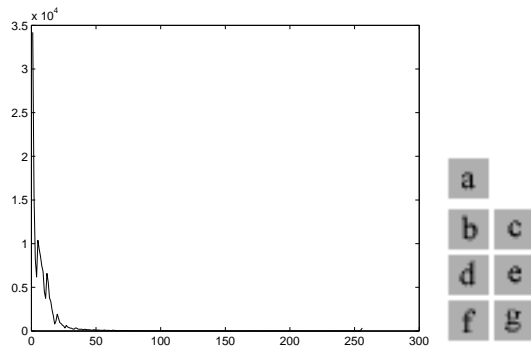


Figure 4.18: Cell Clusters. “px6.jpg” manually cropped to a region of interest before segmentation. (a) image histogram, (b) original image, (c) Otsu, (d) k -means, (e) FCM, (f) Geostatistical ($h = 1$), (g) Geostatistical (mean of $h = 1, 2$, and 3)

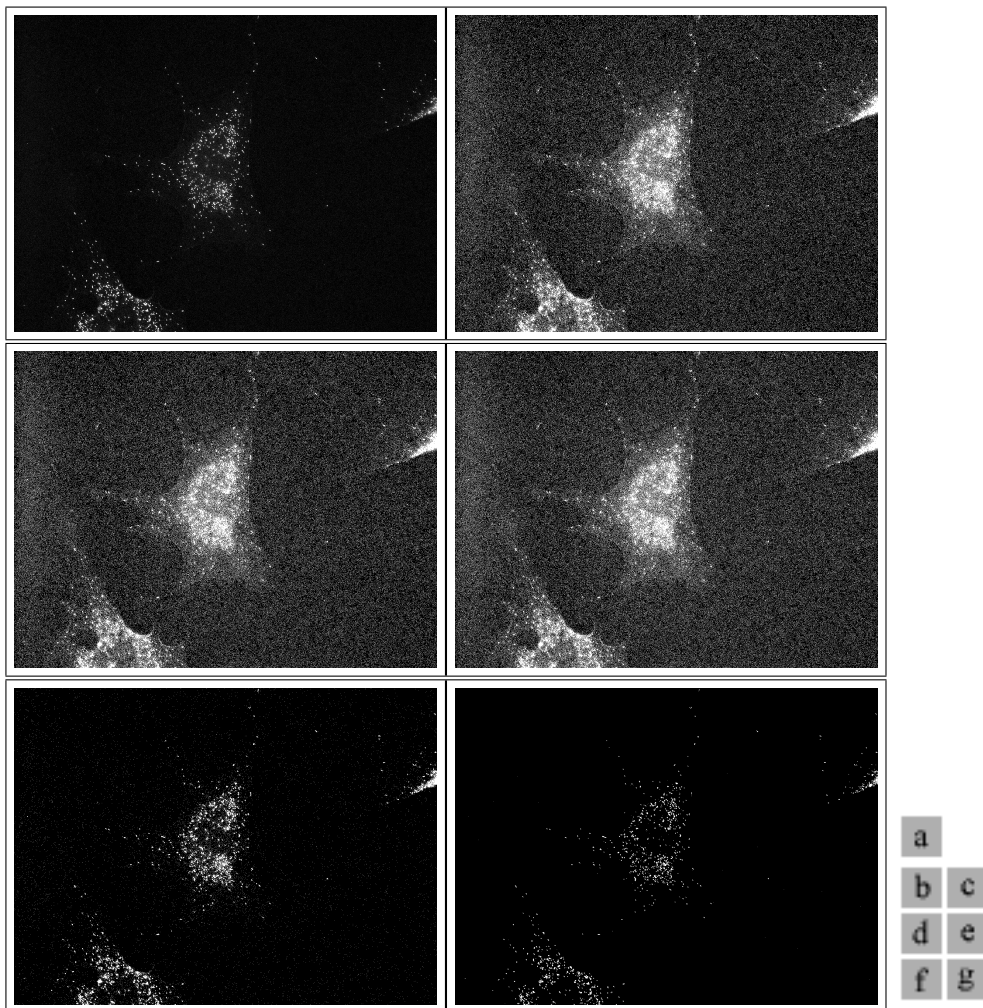
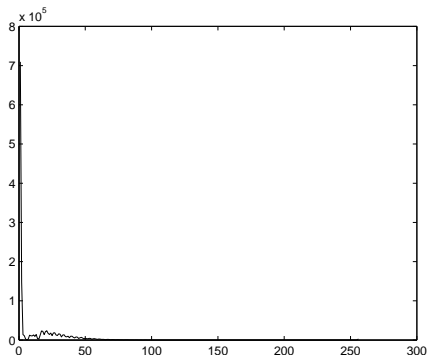


Figure 4.19: Cell Clusters. “px7.jpg” (a) image histogram, (b) original image, (c) Otsu, (d) k -means, (e) FCM, (f) Geostatistical ($h = 1$), (g) Geostatistical (mean of $h = 1, 2$, and 3)

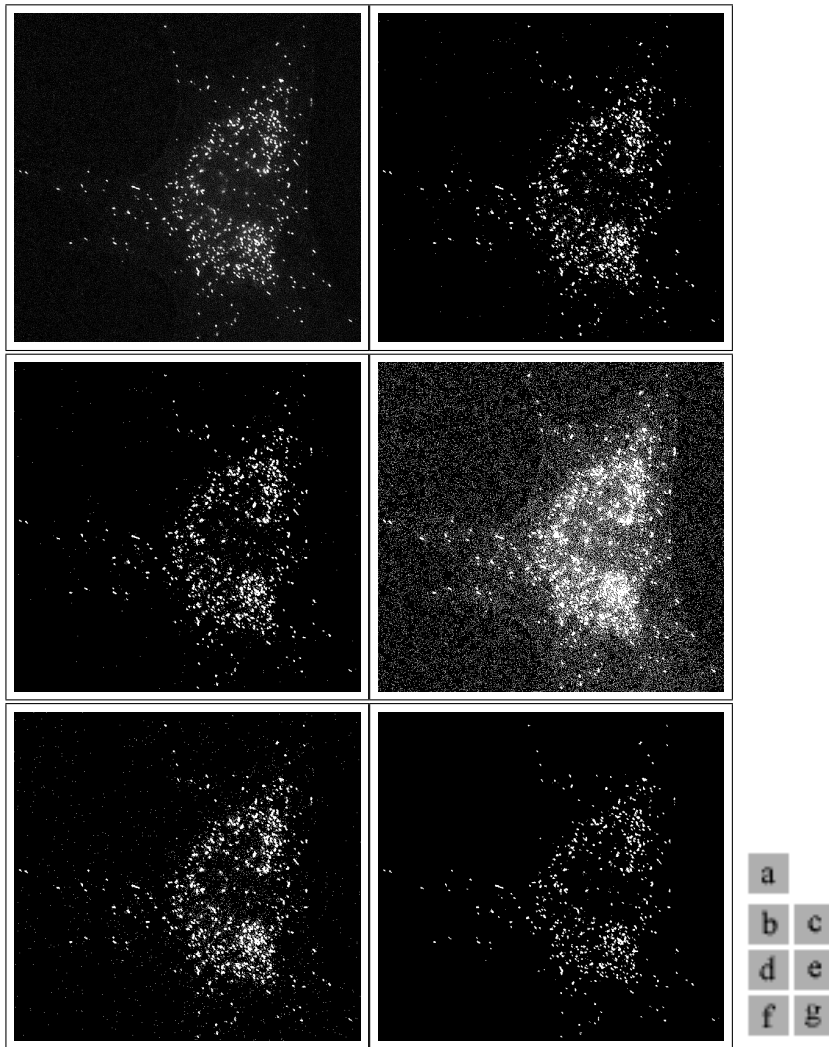
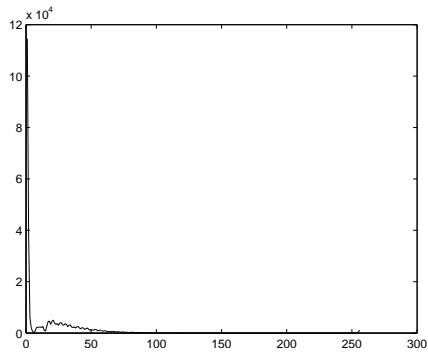


Figure 4.20: Cell Clusters. “px7.jpg” manually cropped to a region of interest before segmentation. (a) image histogram, (b) original image, (c) Otsu, (d) k -means, (e) FCM, (f) Geostatistical ($h = 1$), (g) Geostatistical (mean of $h = 1, 2$, and 3)

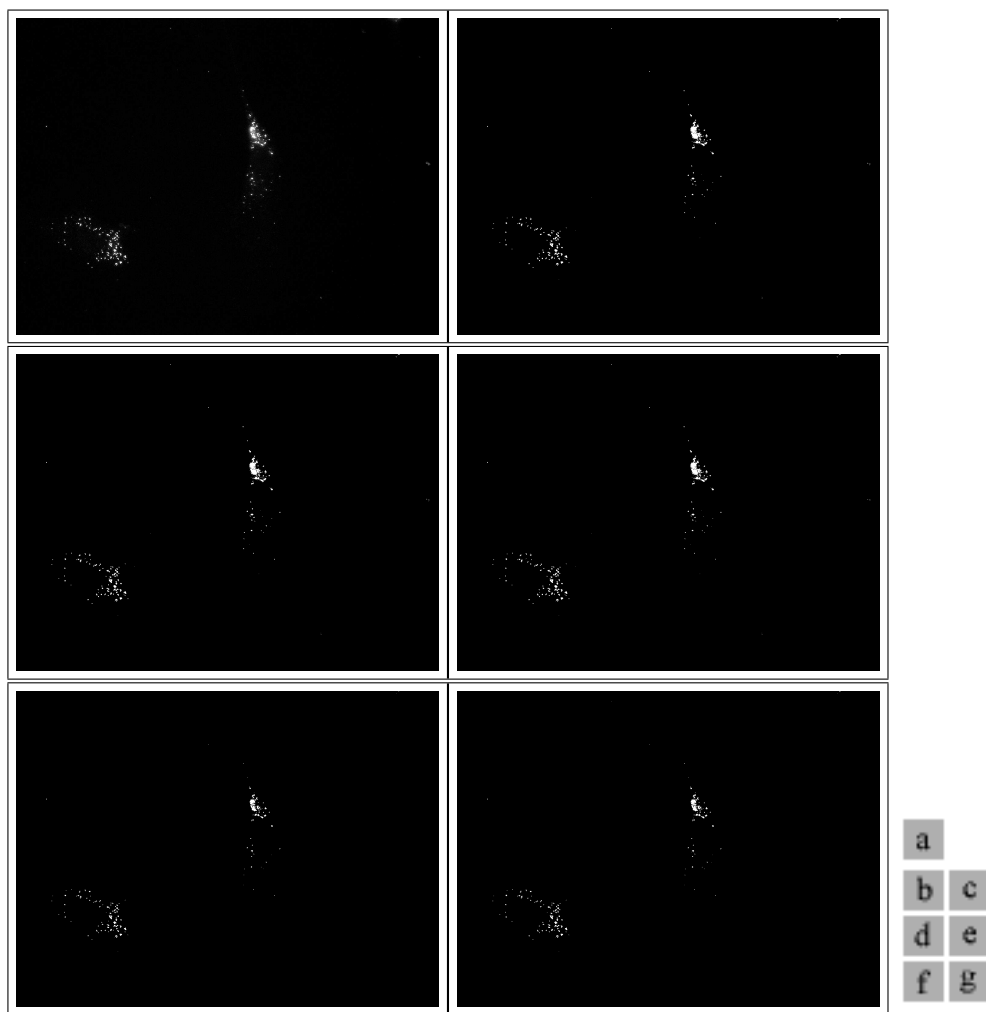
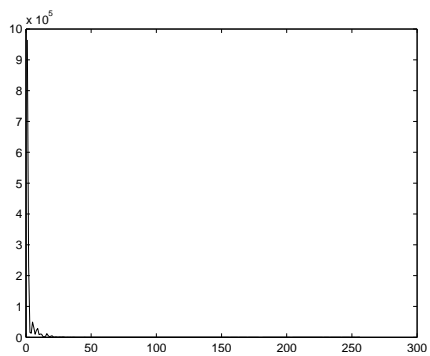


Figure 4.21: Cell Clusters. “px8.jpg” (a) image histogram, (b) original image, (c) Otsu, (d) k -means, (e) FCM, (f) Geostatistical ($h = 1$), (g) Geostatistical (mean of $h = 1, 2$, and 3)

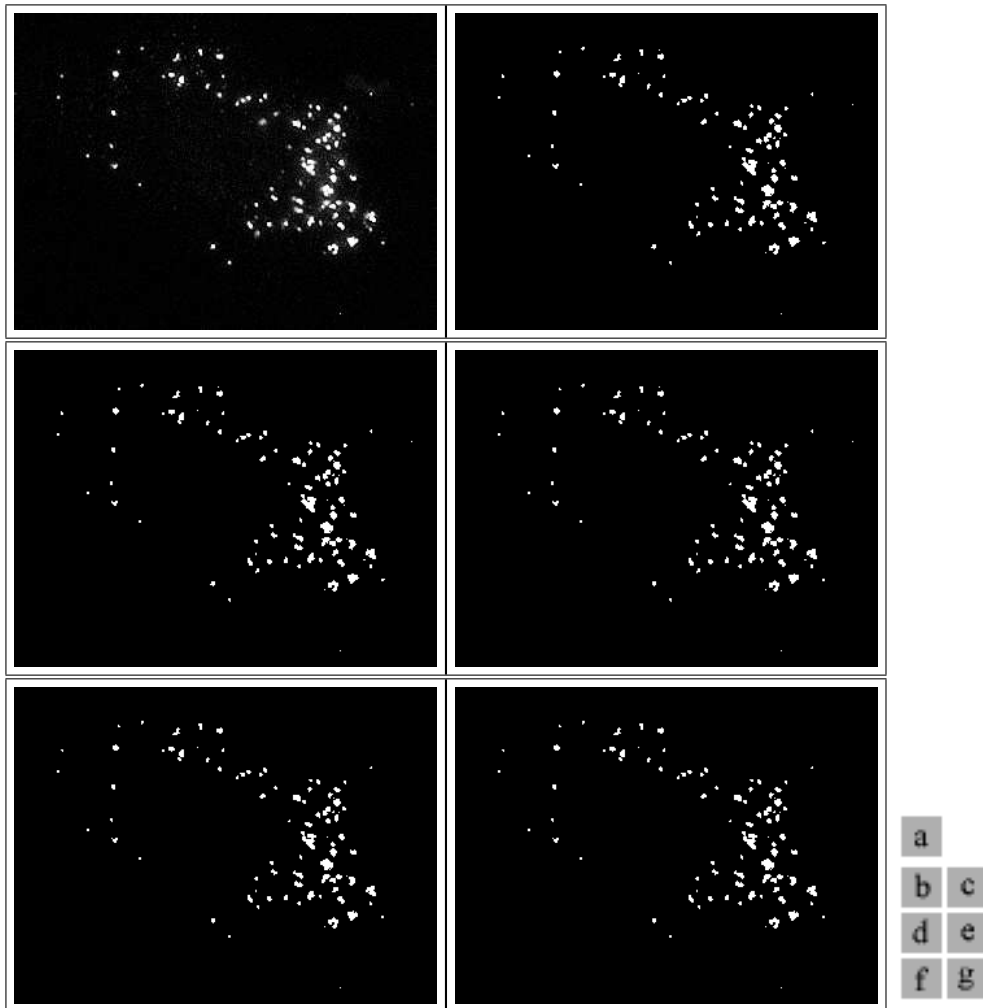
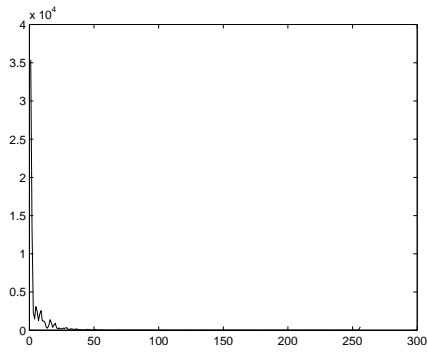


Figure 4.22: Cell Clusters. “px8.jpg” manually cropped to a region of interest before segmentation. (a) image histogram, (b) original image, (c) Otsu, (d) k -means, (e) FCM, (f) Geostatistical ($h = 1$), (g) Geostatistical (mean of $h = 1, 2$, and 3)

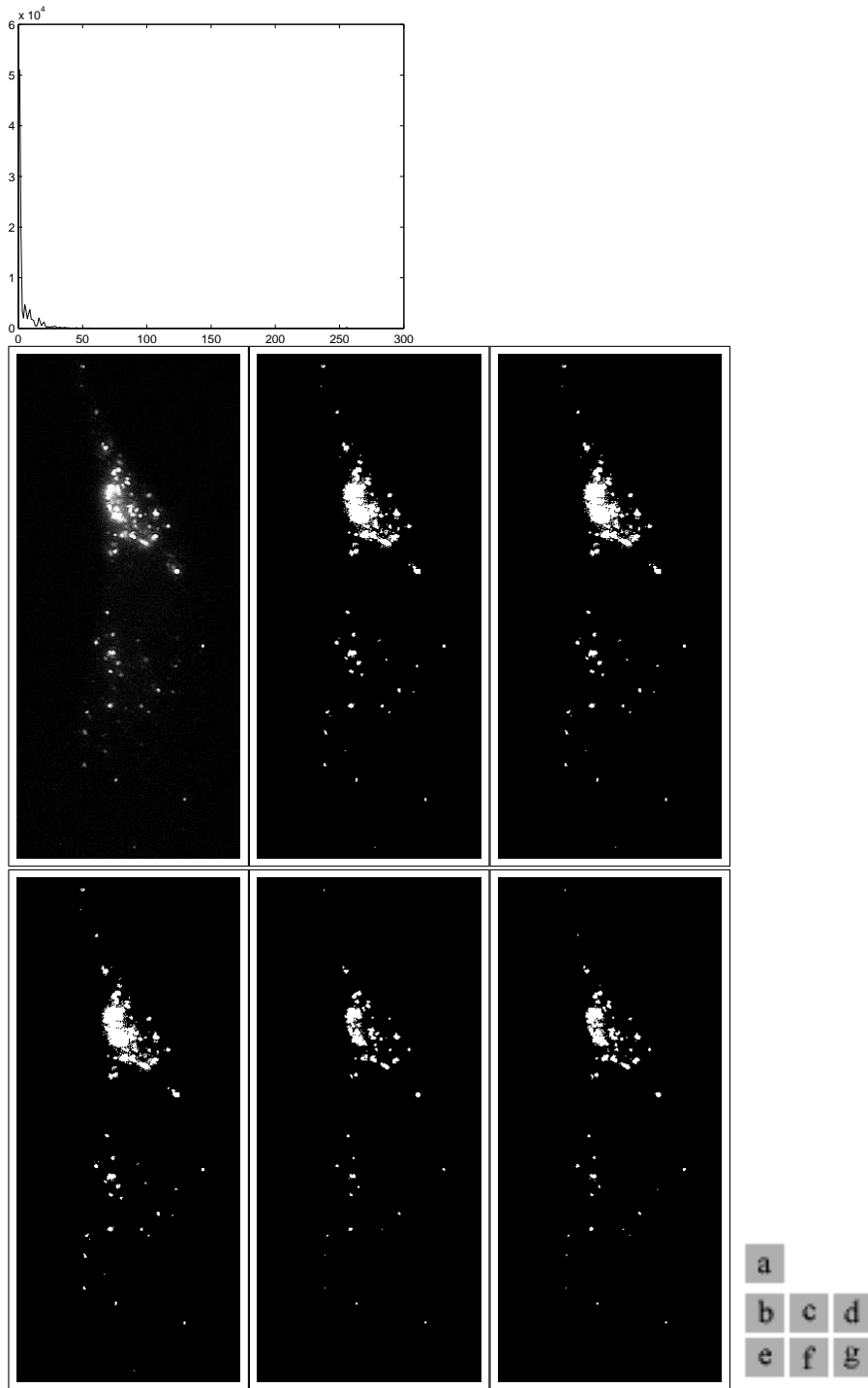


Figure 4.23: Cell Clusters. “px8.jpg” manually cropped to a region of interest before segmentation. (a) image histogram, (b) original image, (c) Otsu, (d) k -means, (e) FCM, (f) Geostatistical ($h = 1$), (g) Geostatistical (mean of $h = 1, 2$, and 3)

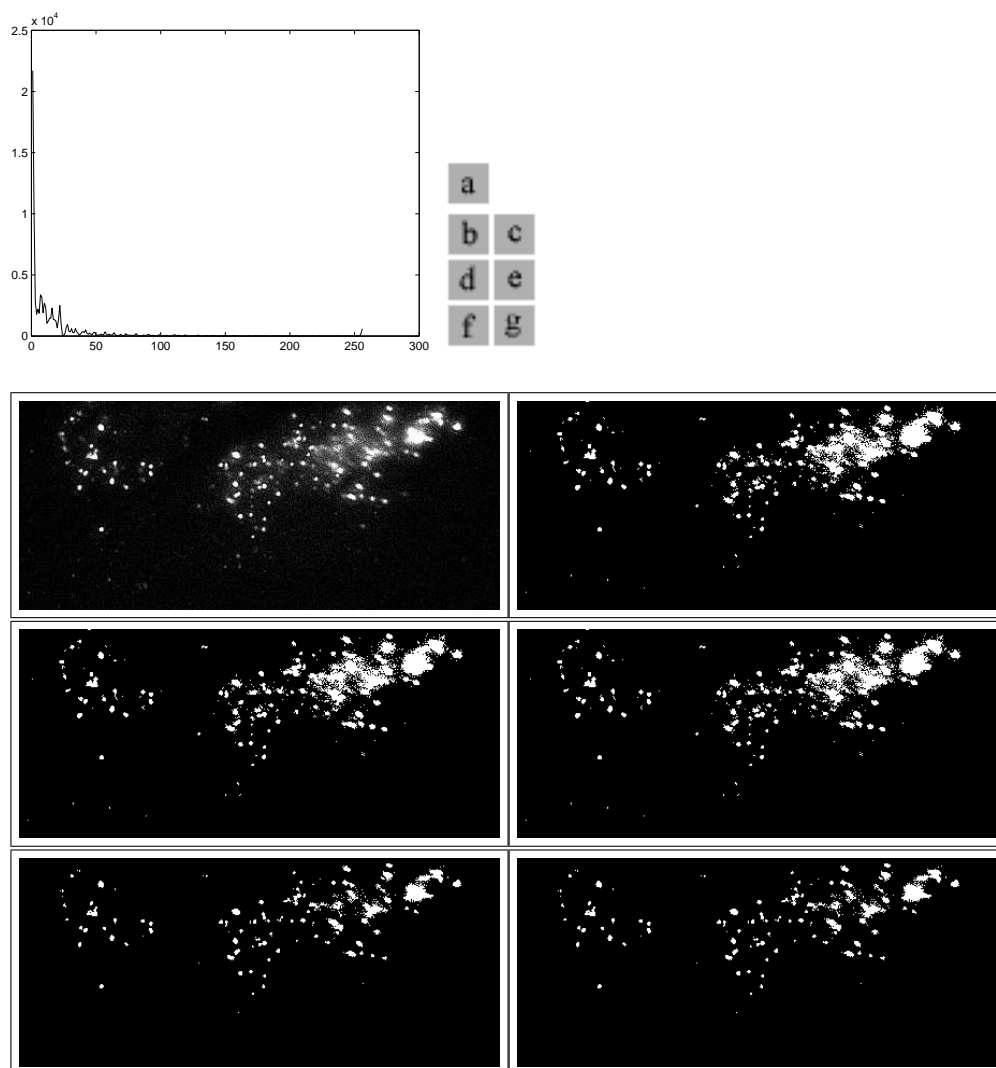


Figure 4.25: Cell Clusters. “px9.jpg” manually cropped to a region of interest before segmentation. (a) image histogram, (b) original image, (c) Otsu, (d) k -means, (e) FCM, (f) Geostatistical ($h = 1$), (g) Geostatistical (mean of $h = 1, 2$, and 3)

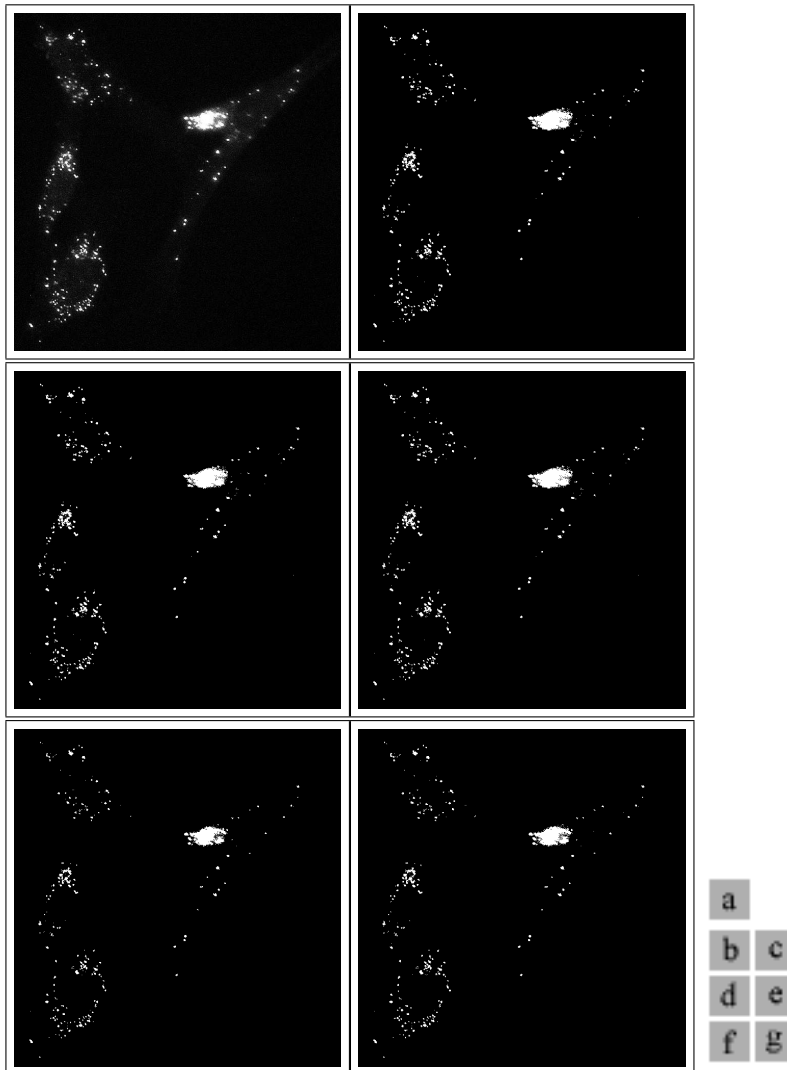
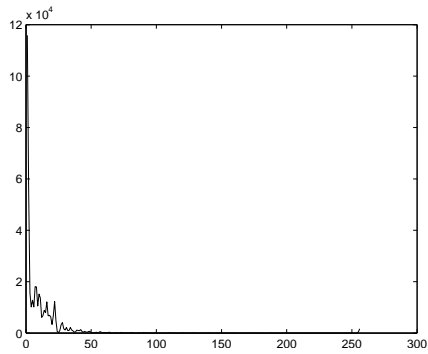


Figure 4.26: Cell Clusters. “px9.jpg” manually cropped to a region of interest before segmentation. (a) image histogram, (b) original image, (c) Otsu, (d) k -means, (e) FCM, (f) Geostatistical ($h = 1$), (g) Geostatistical (mean of $h = 1, 2$, and 3)

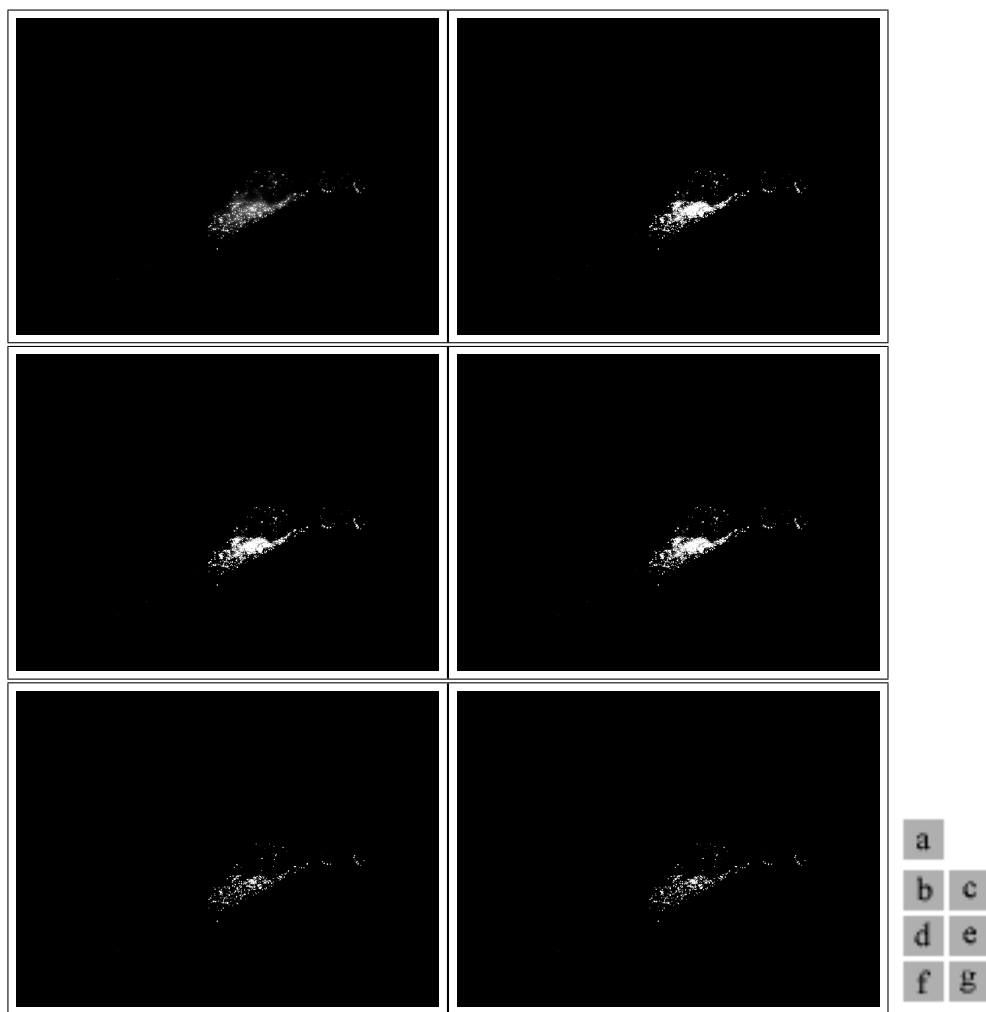
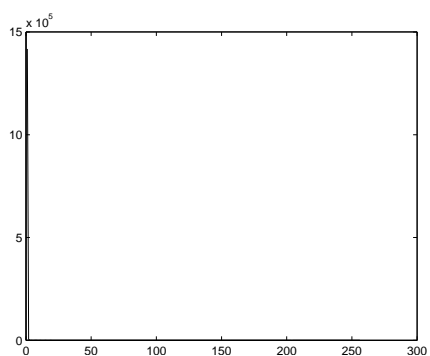


Figure 4.27: Cell Clusters. “px10.jpg” (a) image histogram, (b) original image, (c) Otsu, (d) k -means, (e) FCM, (f) Geostatistical ($h = 1$), (g) Geostatistical (mean of $h = 1, 2$, and 3)

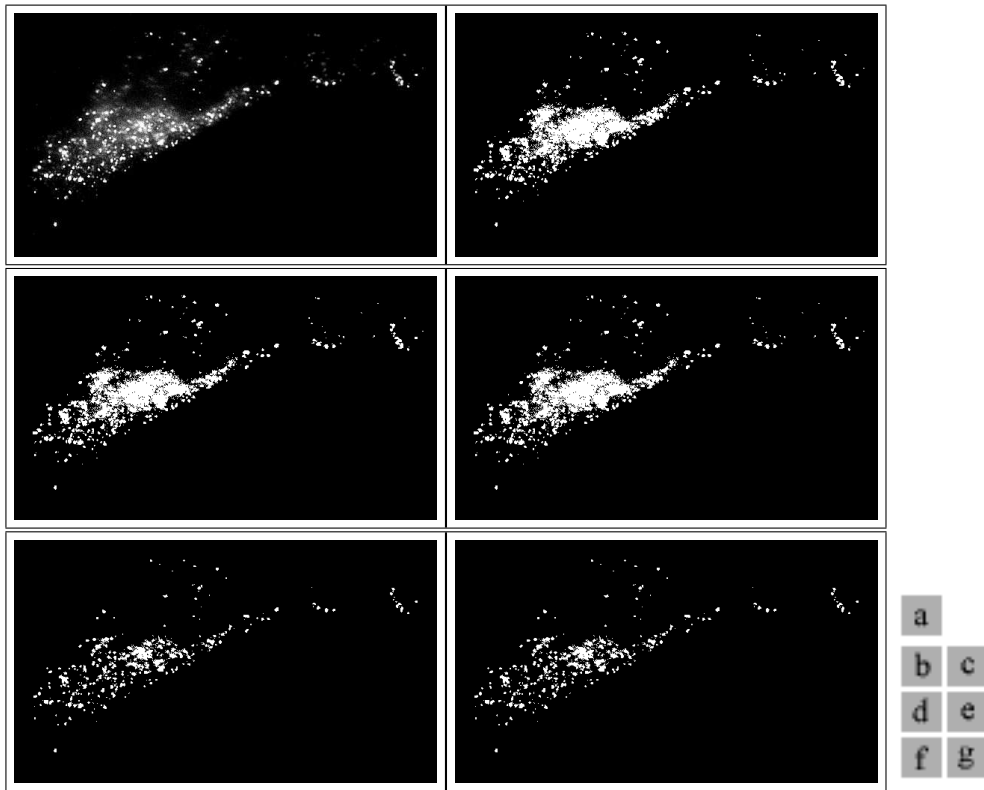
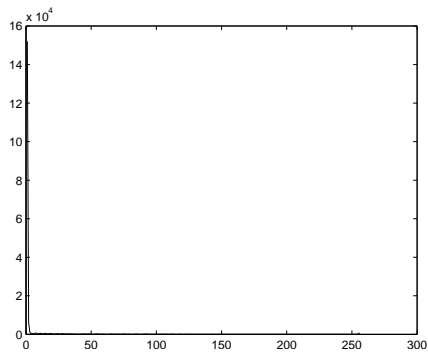


Figure 4.28: Cell Clusters. “px10.jpg” manually cropped to a region of interest before segmentation. (a) image histogram, (b) original image, (c) Otsu, (d) k -means, (e) FCM, (f) Geostatistical ($h = 1$), (g) Geostatistical (mean of $h = 1, 2$, and 3)

As can be seen in Figure 4.29, analysis by histogram statistics alone can fail in the case where one of the classes is statistically insignificant, especially if the majority class displays characteristics utilised by the segmentation algorithm. For example, Otsu’s between-class threshold divides a bimodal histogram at the trough. If an image contains a statistically insignificant foreground class, and the background class is itself bimodal, Otsu’s threshold will ignore the foreground object and segment the background accordingly.

Similarly, the clustering techniques have in this case completely disregarded the foreground pixels as insignificant, and produced segmentations 1 level different from Otsu’s threshold. While the tight grouping of results may suggest that these techniques are correct, it is readily apparent when looking at the images that they are in fact wrong, all to the same degree, and therefore, probably, in the same way.

Spatial analysis overcomes the problem of discounting statistically insignificant classes by effectively treating the image as 3-dimensional, incorporating its 2-dimensional structure as well as intensity into calculations. As such, statistically insignificant but regionally significant data are not discounted.

Figures 4.30 to 4.34 demonstrate the difficulties still apparent when segmenting extremely complex images, with blurriness, noise, and intensity inhomogeneities, such as retinal images. It can be seen in the original images (*b* throughout) that parts of the background are actually darker than the foreground, causing the same problem as that experienced in MR images with intensity inhomogeneities. All the techniques implemented in this document will fail in this situation.

As mentioned elsewhere, in sections 1.2.3 and 5.1, methods have been pro-

posed to improve the effectiveness of thresholding and FCM in the presense of noise and intensity inhomogeneities [13, 12, 29]. It should be noted that the solution provided by the FCM techniques requires or emulates inclusion of spatial information into the FCM calculations — a solution parallelling the geostatistical threshold. Additionally other methods not derived from these classic techniques have been proposed[29, pp. 600-626]. However work still remains to be done before a generally effective technique is devised for segmenting retinal images.

Figure **4.30** clearly demonstrates the effect of using broader lag distances in calculating geostatistical thresholds. Image (f) shows a much smaller foreground classification, resulting in a cleaner distinction between objects and background, than image (g) because (f) uses a smaller lag distance (a tighter region) to calculate its semivariogram. The gaps in the veins of image (f) are not a problem as techniques exist to fill them, such as described by Alonso-Montes *et. al.*[30]. Also, it is apparent by comparing Figures **4.30** and **4.34** that the determination of an optimal lag distance (or range of lag distances) is image dependant.

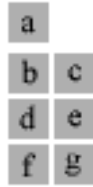
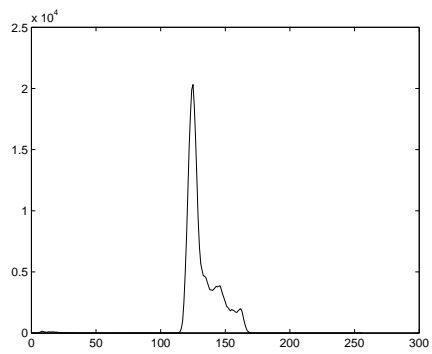


Figure 4.29: Helicopter. “image3.bmp” (a) image histogram, (b) original image, (c) Otsu, (d) k -means, (e) FCM, (f) Geostatistical ($h = 1$), (g) Geostatistical (mean of $h = 1, 2$, and 3)

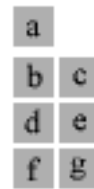
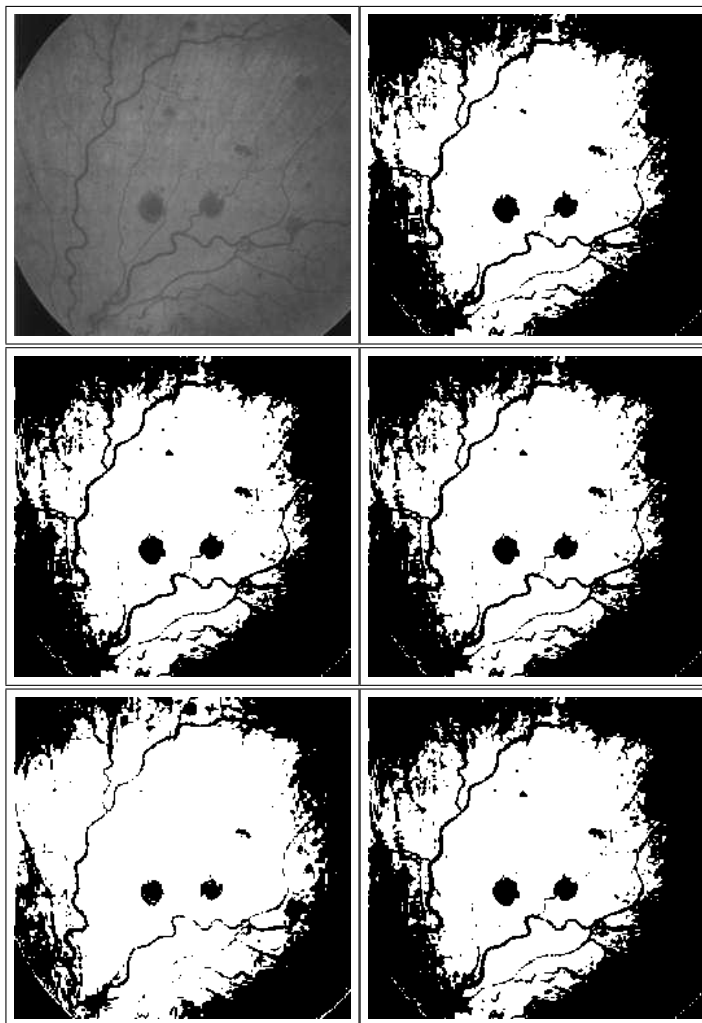
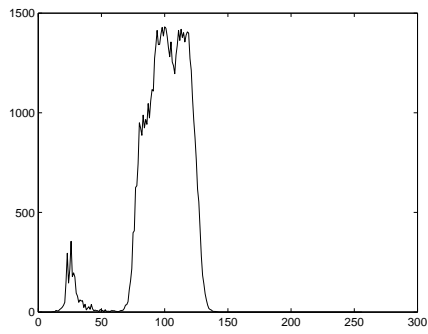


Figure 4.30: Retina. “Diabetes-haem.jpg” (a) image histogram, (b) original image, (c) Otsu, (d) k -means, (e) FCM, (f) Geostatistical ($h = 1$), (g) Geostatistical (mean of $h = 1, 2$, and 3)

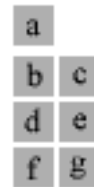
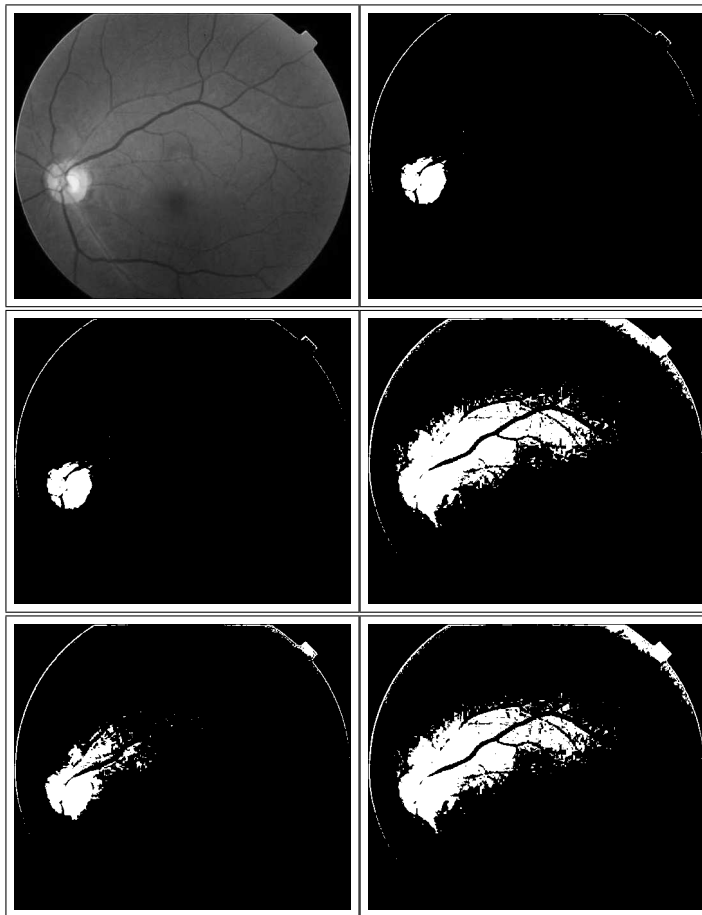
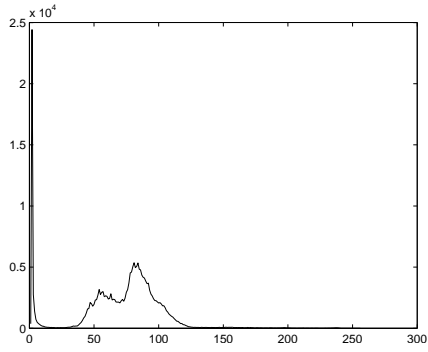


Figure 4.31: Retina. “Mitam_A.jpg” (a) image histogram, (b) original image, (c) Otsu, (d) k -means, (e) FCM, (f) Geostatistical ($h = 1$), (g) Geostatistical (mean of $h = 1, 2$, and 3)

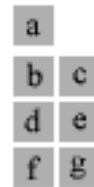
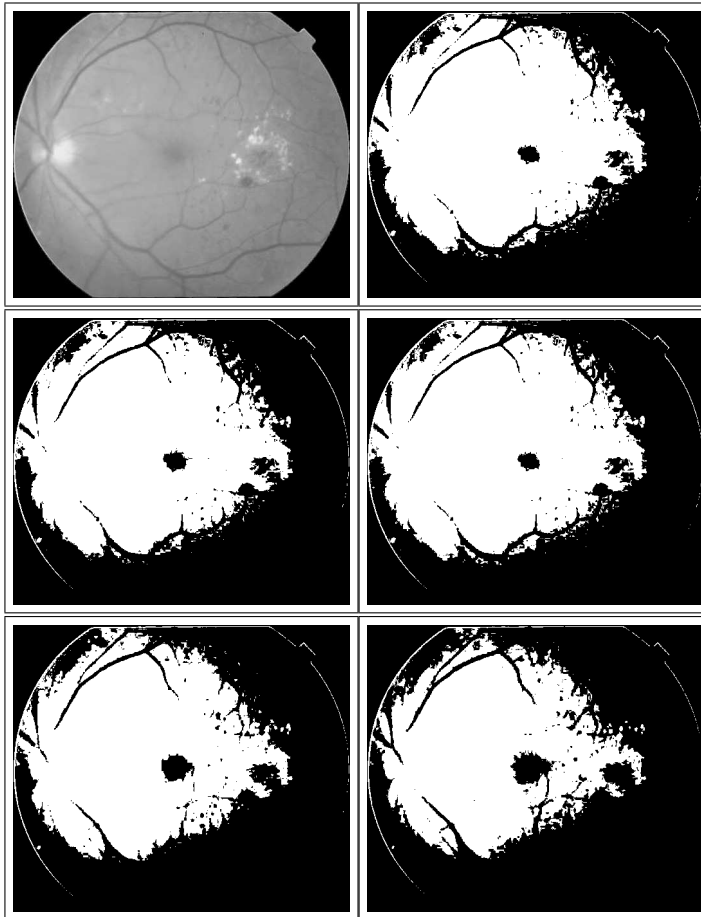
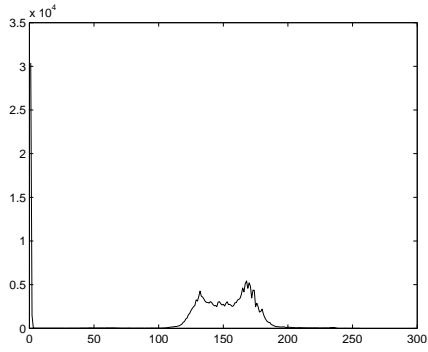


Figure 4.32: Retina. “Mitam.B.jpg” (a) image histogram, (b) original image, (c) Otsu, (d) k -means, (e) FCM, (f) Geostatistical ($h = 1$), (g) Geostatistical (mean of $h = 1, 2$, and 3)

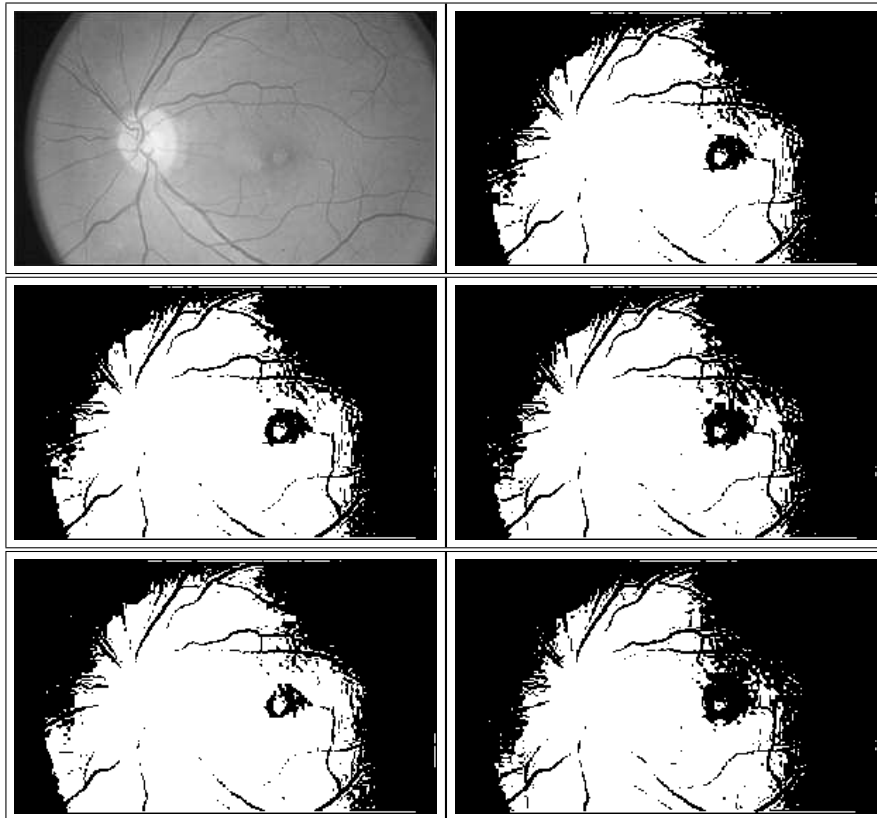
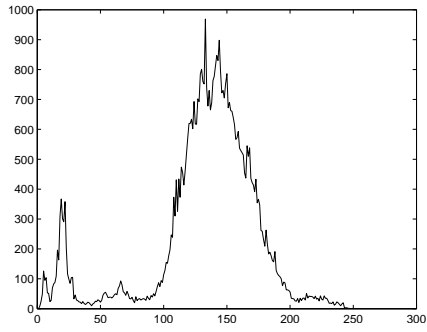


Figure 4.33: Retina. “Eye-1-normal.jpg” (a) image histogram, (b) original image, (c) Otsu, (d) k -means, (e) FCM, (f) Geostatistical ($h = 1$), (g) Geostatistical (mean of $h = 1, 2$, and 3)

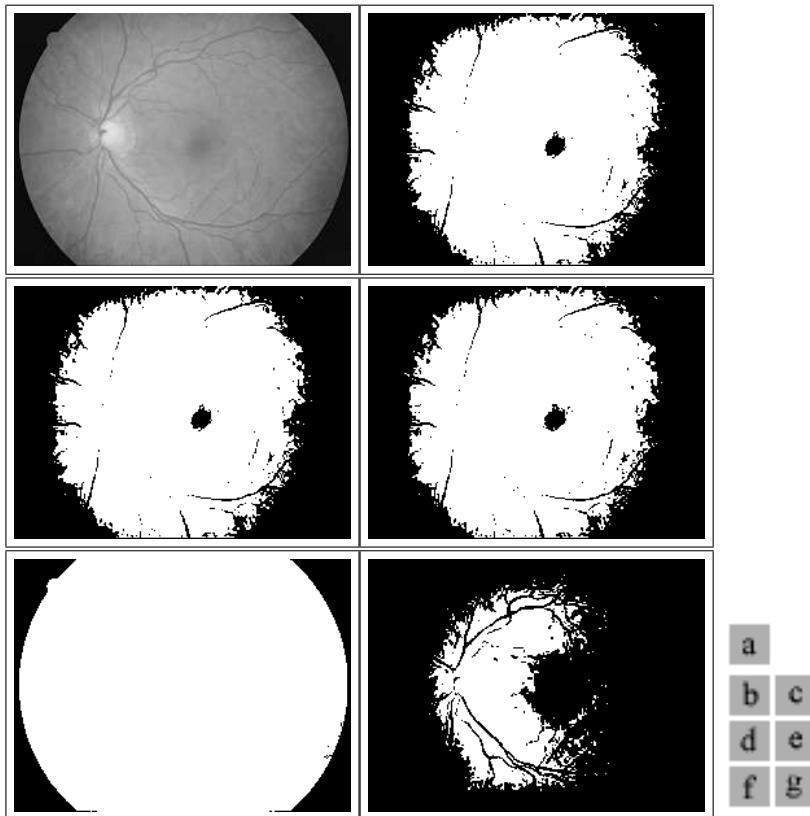
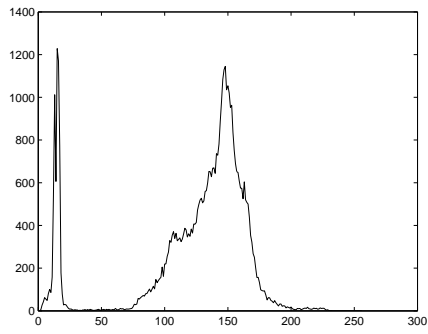


Figure 4.34: Retina. “Eye-2-normal.jpg” (a) image histogram, (b) original image, (c) Otsu, (d) k -means, (e) FCM, (f) Geostatistical ($h = 1$), (g) Geostatistical (mean of $h = 1, 2, \text{ and } 3$)

FILENAME	Otsu	<i>k</i> -means	FCM	Geo. ^(h=1)	Geo. ^(h=1,...,3)
cameraman.tif	88	89	90	116	116
rice.tif	125	126	127	126	126
shot1.tif	174	175	176	117	117
tissue1.tif	131	132	132	126	126
nodules1.tif	148	149	149	145	146
image3.bmp	135	136	136	73	69
image4.bmp	133	219	129	120	127
imageA.jpg	62	62	64	89	89
imageB.jpg	56	56	56	101	96
imageC.jpg	49	50	51	72	67
imageD.jpg	61	62	63	84	84
imageE.jpg	58	59	14	91	87
image_5min.jpg	166	173	174	178	178
image_15min.jpg	174	177	182	180	194
image_30min.jpg	182	184	187	203	203
image_60min.jpg	189	191	193	188	220
image_120min.jpg	178	191	191	183	182
image_180min.jpg	172	174	178	175	175
px3_crop1.jpg	94	95	19	154	139
px5_crop1.jpg	44	45	41	153	126
px6_crop1.jpg	106	107	109	157	147
px6_crop2.jpg	87	88	89	160	151
px7_crop1.jpg	91	91	34	76	121
px8_crop1.jpg	109	110	112	124	124
px8_crop2.jpg	84	85	87	155	138
px9_crop1.jpg	84	85	86	137	137
px9_crop2.jpg	104	104	107	143	129
px10_crop1.jpg	72	75	75	139	139
px1.jpg	89	90	91	159	144
px2.jpg	100	14	14	8	152
px3.jpg	51	52	52	9	94
px4.jpg	76	76	74	147	127
px5.jpg	67	67	64	147	118
px6.jpg	90	11	11	3	148
px7.jpg	26	25	23	65	121
px8.jpg	94	95	97	137	130
px9.jpg	94	95	96	142	138
px10.jpg	71	72	73	142	141
Diabetes-haem.jpg	101	102	102	96	102
Eye-1-normal.jpg	141	141	143	139	145
Eye-2-normal.jpg	132	132	133	72	155
Mitam_A.jpg	127	128	99	112	100
Mitam_B.jpg	152	153	152	157	161

Table 4.1: Threshold values for each segmentation technique, presented in the range (0...255).

4.1 Discussions

The k -means and FCM segmentation techniques appear to have difficulty segmenting properly in the presence of noise. This problem can be overcome by analysing the spatial structure of image data, rather than intensity data alone.

According to spatial analysis, isolated points (noise) are deemed less significant, and so have very little effect on the resulting segmentation. By discounting spatial information it is impossible to determine if a particular datum should be discounted as noise.

As apparent in Table 4.1, geostatistical thresholding tends to produce thresholds farther from the background. That is, when the background is dark, the threshold is higher; when the background is light, the threshold is lower. This reduces the number of pixels classified as “foreground,” in turn reducing the size of segmented objects, improving contrast between objects, as well as reducing rough edges and noise in the segmented images. This is particularly useful in case of blurriness or staining in the original image, as only high-membership object pixels are classified as such.

It can also be seen that in images with a vast majority of pixels in one class, especially when that class can itself be determined as bimodal, as in Figure 4.29, Otsu’s thresholding method and the two clustering algorithms can fail entirely to account for any distinction between the ‘real’ classes, even where such distinction may seem obvious to a human user.

Finally, it is apparent that retinal images are universally hard to segment using any of the techniques specified in this document.

Chapter 5

Conclusions

Image segmentation remains an important field of research, particularly with applications in bioinformatics — using computers to aid in diagnosis of pathologies or analyse effects of different treatments, allowing for faster turnarounds and higher throughput of data in situations that are very significant sociologically.

Throughout this document the reader has been exposed to many image segmentation methods, such as thresholding, clustering, and region-based techniques, among others. Many implementation of these techniques have been described in general terms, with links to further research provided if required.

Image segmentation techniques: Otsu's thresholding method, k -means and fuzzy c -means clustering, as well as the recent geostatistical threshold technique, have been explained in detail, and their results compared over many images.

It has been shown that geostatistical thresholding consistently performs better than Otsu's threshold, k -means and fuzzy c -means clustering in the

presence of imperfections such as noise and blurring. As such it can be deduced that structural analysis of an image is too significant to be overlooked when performing segmentation, especially in the case of poor quality (low contrast or noisy) images.

5.1 Suggestions for Further Research

It may be possible to combine the statistical (histogram) analysis of Otsu's threshold with the spatial analysis of the geostatistical threshold, and create a generalised solution that incorporates both statistical and geostatistical analysis.

For example, by dividing the mean variance of a threshold ($\bar{V}(k)$, defined in section 2.3) by the total number of pixels in the image, one would derive a spatially determined within-class variance expressed in a way that is comparable with the within-class variance (σ_W^2) provided by Otsu's thresholding technique, and could be used in place of σ_W^2 in the objective function λ defined in section 1.9.

Additionally, from a theoretical viewpoint and evidenced in Figures 4.30 to 4.34, it is apparent that non-uniform images and intensity inhomogeneities produce a situation in which foreground and background classes are not linearly separable, so any technique based on the assumption of linear separability (such as thresholding) will fail without modification.

Retinal images have been demonstrated in this document as they have been found to be a common topic of research in available literature, as well as having significant impact on society with the current prevalence of diabetes.[35, 36] Alonso-Montes *et. al.* demonstrate a technique to extract

blood vessels from retinal images[30], however other features may also be of interest to researchers, such as hard and soft exudates, haemorrhages, microaneurysms, and neovascularisation, among others[2], so new techniques or modifications of existing techniques are still required.

One suggestion of modification may be a pre-processing stage, which detects and artificially removes inhomogeneities in an image. Other techniques may involve creating multiple region-based thresholds or segmentations which are combined into an overall segmentation; or adaptive (or non-linear) thresholds.

Gonzalez and Woods have described ways in which adaptive thresholding may be implemented[29, pp. 600-617], along with some apparent problems arising from these techniques, and attempts to resolve these problems. For example, it is suggested that “one approach for improving the shape of histograms is to consider only those pixels that lie on or near the edges between objects and the background,”[29, pg. 608] however this technique requires that one already know the edges between objects and background. Edges may be approximated using gradient/Laplacian calculations, however such approximations will always be unreliable in the presence of blurring or staining in the image.

Other techniques may be devised to utilise the statistical analysis techniques of Otsu’s and the geostatistical thresholds in a non-linearly separable environment. The basic understanding of current image segmentation techniques, as well as the list of references for further study, provided by this document will give researchers a strong base of general knowledge on which to devise new or improved techniques.

Bibliography

- [1] Framme, C., Roider, J., Sachs, H.G., Brinkmann, R., Gabel, V. (2004) “Noninvasive Imaging and Monitoring of Retinal Pigment Epithelium Patterns Using Fundus Autofluorescence - Review” *Current Medical Imaging Reviews*, 2005, 1, pp. 89-103.
- [2] Mitamura, Y., Harada, C., Harada, T. (2004) “Role of Cytokines and Trophic Factors in the Pathogenesis of Diabetic Retinopathy” *Current Diabetes Reviews*, 2005, 1, pp. 73-81.
- [3] Newsom, R.S.B., Clover, A., Costen, M.T.J., Sadler, J., Newton, J., Luff, A.J., Canning, C.R. (2001) “Effect of digital image compression on screening for diabetic retinopathy” *Br. J. Ophthalmol.* 2001, 85, pp. 799-802.
- [4] Otsu, N. (1979) “A Threshold Selection Method from Gray-Level Histograms”, *IEEE Trans. Syst., Man, Cybern.* 9 (1), pp. 62-69.
- [5] Tobias, O.J., Seara, R. (2002) “Image Segmentation by Histogram Thresholding Using Fuzzy Sets”, *IEEE Trans. Image Processing.* 11 (12), pp. 1457-1465.

- [6] Kaufmann, A. (1975) *"Introduction to the Theory of Fuzzy Subsets"*, New York: Academic Press, New York.
- [7] De Luca, A., Termini, S. (1972) "A Definition of a Nonprobabilistic Entropy in the Setting of Fuzzy Set Theory", *Inform. and Control.* 20, pp. 301-312.
- [8] Chi, Z., Yan, H., Pham, T. (1996) "Fuzzy Algorithms: With Applications to Image Processing and Pattern Recognition", *Advances in Fuzzy Systems — Applications and Theory Vol. 10*, World Scientific Publishing Co., Singapore.
- [9] Ball, G.H., Hall, D.J. (1965) *"ISODATA: A Novel Method of Data Analysis and Pattern Classification"*, Stanford Res. Inst., Menlo Park, California.
- [10] Dunn, J.C. (1973): "A Fuzzy Relative of the ISODATA Process and Its Use in Detecting Compact Well-Separated Clusters", *J. Cybernet.* 3, pp. 32-57.
- [11] Bezdek, J.C. (1981): *"Pattern Recognition with Fuzzy Objective Function Algorithms"*, Plenum Press, New York.
- [12] Lei Jiang, Wenhui Yang (2003) "A Modified Fuzzy C-Means Algorithm for Segmentation of Magnetic Resonance Images", *Proc. VIIth Digital Image Computing: Techniques and Applications*, pp. 225-232.
- [13] Dao-Qiang Zhang, Song-Can Chen (2004) "A Novel Kernelized Fuzzy C-Means Algorithm With Application In Medical Image Segmentation", *Artif. Intell. Med.* 32 (1), pp. 37-50.

- [14] Songül Albayrak, Fatih Amasyalı(2003) “Fuzzy C-Means Clustering On Medical Diagnostic Systems”, *International XII. Turkish Symposium on Artificial Intelligence and Neural Networks*.
- [15] Hamerly, G., Elkan, C. (2002) “Alternatives to the k-Means Algorithm That Find Better Clusterings”, *CIKM '02*, pp. 600-607.
- [16] Osareh, A., Mirmehdi, M., Thomas, B., Markham, R. (2001) “Automatic Recognition of Exudative Maculopathy Using Fuzzy C-Means Clustering and Neural Networks”, *Medical Image Understanding and Analysis (ed. E. Claridge, J. Bamber)*, BMVA Press, pp. 49-52.
- [17] Pham, D.L., Prince, J.L. (1998) “An Adaptive Fuzzy C-Means Algorithm for Image Segmentation in the Presence of Intensity Inhomogeneities”, *Proc. SPIE Medical Imaging 1998: Image Processing*, 3338, pp. 555-563.
- [18] Pham, D.L., Chenyang Xu, Prince, J.L. (2000) “Current Methods in Medical Image Segmentation”, *Annu. Rev. Biomed. Eng.*, pp. 315-337.
- [19] Zadeh, L.A. (1973) “Outline of a New Approach to the Analysis of Complex Systems and Decision Processes”, *IEEE Trans. Syst., Man, Cybern.* 3 (1), pp. 28-44.
- [20] Zhang, B., Hsu, M., Dayal, U. (1999) “K-harmonic means — a data clustering algorithm” *Technical Report HPL-1999-124, Hewlett-Packard Labs*.
- [21] Zhang, B. (2000) “Generalized k-harmonic means — boosting unsupervised learning” *Technical Report HPL-2000-137, Hewlett-Packard Labs*.

- [22] Matheron, G. (1962) “*Trait de gostatistique applique*”, Tome 1, Editions Technip, Paris.
- [23] Clark, I., (1979) “*Practical Geostatistics*”, Applied Science Publishers Ltd., Essex.
- [24] Royle, A.G., (1980) “Why Geostatistics?” Chapter 1 of *Geostatistics*, McGraw-Hill Inc., New York, pp. 1-16.
- [25] Clark, I., (1980) “The Semivariogram.” Chapters 2-3 of *Geostatistics*, McGraw-Hill Inc., New York, pp. 17-40.
- [26] Pham, T.D. (2003) “Applications of geostatistics and Markov models for logo recognition”, *Proc. SPIE-IS&T. 5010*, pp. 20-27.
- [27] Pham, T.D. (2003) “Variogram-based feature extraction for neural network recognition of logos”, *Pro. SPIE. 5015*, pp. 22-29.
- [28] Allard, D. (1998) “Geostatistical Classification and Class Kriging”, *Journal of Geographic Information and Decision Analysis. 2 (2)*, pp. 77-90.
- [29] Gonzalez, R.C., Woods, R.E. (2002) “*Digital Image Processing*”, Prentice-Hall Inc., New Jersey.
- [30] Alonso-Montes, C., Vilariño, D.L., Penedo, M.G. (2005) “On the Automatic 2D Retinal Vessel Extraction” *ICAPR 2005, LNCS 3687*, pp. 165-173.
- [31] Bloch, I. (1994) “Fuzzy Sets In Image Processing”, *Symposium on Applied Computing*, pp. 175-179.

- [32] Keller, J.M., Gray, M.R., Givens, J.A. JR. (1985) "A Fuzzy K-Nearest Neighbor Algorithm", *IEEE Trans. Syst., Man, Cybern.* 15 (4), pp. 580-585.
- [33] Zadeh, L.A. (1965) "Fuzzy Sets", *Inform. Control*, 8, pp. 338-353.
- [34] Sahoo, P.K., Soltani, S., Wong, A.K.C. (1988) "A survey of thresholding techniques" *Comput. Vis. Graph. Image Proc.* 41, pp. 233-60.
- [35] Abbate, S., Martin, W., Twillman, G. [Ed] (2002) "*Diabetes & Cardiovascular Disease Review*" Issue 2; American Diabetes Association / American College of Cardiology, Virginia.
- [36] Wilde, B. (2002) "*Diabetes Facts*" Downloaded from <http://www.diabetesaustralia.com.au> Sep 2005.